2020-02-01

Noise Reduction of EEG Signals Using Autoencoders Built Upon GRU based RNN Layers

Esra Aynali
Technological University Dublin

Noise Reduction of EEG Signals Using Autoencoders Built Upon GRU based RNN Layers

Esra Aynalı

A dissertation submitted in partial fulfilment of the requirements of
Technological University Dublin for the degree of
M.Sc. in Computer Science (Data Analytics)

January 2020

I certify that this dissertation which I now submit for examination for the award of MSc in Computing (Data Analytics), is entirely my own work and has not been taken from the work of others save and to the extent that such work has been cited and acknowledged within the test of my work.

This dissertation was prepared according to the regulations for postgraduate study of the Technological University Dublin and has not been submitted in whole or part for an award in any other Institute or University.

The work reported on in this dissertation conforms to the principles and requirements of the Institute's guidelines for ethics in research.

Signed: **Esra Aynalı**

Date: **26 January 2020**

ABSTRACT

Understanding the cognitive and functional behaviour of brain by its electrical activity is an interesting area. Electroencephalography (EEG) is a method that measures and record electrical activities in the brain. It has been used for pathology analysis, emotion recognition, clinical and cognitive research, diagnosing various neurological and psychiatric disorders and other applications. Since the EEG signals are sensitive to activities other than the brain activities such as eye blinking, eye movement, head movement, etc., and it is not possible to record EEG signals without any noise, it is very important to use an efficient noise reduction technique to get more accurate results. Numerous traditional techniques such as Principal Component Analysis (PCA), Independent Component Analysis (ICA), wavelet transformations and machine learning techniques were proposed for reducing the noise in EEG signals. The aim of this paper is to investigate the effectiveness of stacked autoencoders built upon Gated Recurrent Unit (GRU) based Recurrent Neural Network (RNN) layers (GRU-AE) against PCA. To achieve this, Harrell-Davis decile values for the reconstructed signals' signal-to-noise ratio distributions were compared and it was found that the GRU-AE outperformed PCA for noise reduction of EEG signals.

Key words: *ERP, electroencephalography, autoencoders, noise reduction, RNN, GRU, signal-to-noise ratio*

ACKNOWLEDGEMENTS

I would like to express my sincere thanks to my supervisor Dr. Luca Longo for his guidance throughout the whole dissertation process, providing solutions to any kind of problem and for his valuable time and patience.

I would also like to acknowledge and convey my thanks to the Technological University Dublin staff that have assisted me throughout my time in the university, especially to Dr. Robert Ross for providing me an access to the servers to complete my training part.

I would also like to thank Conor Hanrahan and Alexander Suvorov for sharing their work with me to speed up my understanding about the topic and help me to gain insights.

Lastly, love and appreciation to my family and Kemal Araz for supporting me and believing in me.

TABLE OF CONTENTS

TABLE OF FIGURES

TABLE OF TABLES

1. INTRODUCTION

Brain is the most important organ that controls the entire body. It can be considered as a collection of interconnected neurons. Understanding the cognitive and functional behaviour of brain by its electrical activity is an interesting area. Electroencephalography (EEG) is a method that measure and record electrical activities in the brain. First human EEG was recorded by Hans Berger, a German psychiatrist, in 1924 (Haas, 2003). EEG signals demonstrate the condition of the brain, they are widely used in neuroscience and psychophysiological research. It helps researchers to understand how the brain works, which region of the brain is active against the stimulus and how these regions interact with each other.

1.1 Background

EEG signals are the brain rhythm signals from different brain regions. They reflect the activity of the related region (Niedermeyer & da Silva, 2005). They can reveal many important findings about brain. It has been used for pathology analysis, emotion recognition, clinical and cognitive research, diagnosing various neurological and psychiatric disorders such as epilepsy, Alzheimer's disease, memory disorders, sleep disorders, schizophrenia and other applications (Xing, Li, Xu, Shu, Hu & Xu, 2019; Leite, Pereira, Gurjao & Veloso, 2018).

Unlike other existing methods such as Magnetic Resonance Imaging (MRI), Functional Magnetic Resonance Imaging (fMRI) and Computed Tomography (CT), EEG has lower costs. EEG signals can be obtained by electrodes placed on the scalp. It can directly measure neural activity in brain, captures cognitive activity in real-time and in the absence of behavioural responses it can manage cognitive activities. Although these advantages, EEG signals are sensitive to activities other than the brain activities such as eye blinking, eye movement, head movement, etc., and it is not possible to record EEG signals without any noise.

Since the presence of the noise in the EEG signals, numerous traditional techniques such as Principal Component Analysis (PCA), Independent Component Analysis (ICA),

wavelet transformations and machine learning techniques were proposed for reducing the noise in signals to get more accurate results. Although those techniques have some advantages, they also have some drawbacks. For example, those widely used traditional techniques operates under some assumptions about the data and they can perform poorly when the noise in the signal is overlapped or have smaller amplitude and sometimes it is needed to manually identify the noise as a reference.

The aim of this paper is to develop a noise reduction technique that can successfully reduce the noise in the EEG signals while protecting the information in the signal.

1.2 Research Project

Noise in the signals can be measured with the signal-to-noise ratio (SNR). It gives a ratio of the signal power to the noise power present in a signal. Lower SNR indicates that noise in the signal is greater. Noise reduction techniques helps to achieve higher SNRs.

Preserving important information while reducing noise is extremely important for signal processing. Numerous techniques are available for noise reduction such as PCA, ICA and wavelet transformations. Besides those traditional techniques machine learning and deep learning techniques such as stacked autoencoders and convolutional autoencoders became popular for noise reduction. They showed that they significantly increased the SNRs when compared to the traditional techniques.

Since the EEG signals can be treated as timeseries, Long Short Term Memory (LSTM) based Recurrent Neural Network (RNN) and Gated Recurrent Unit (GRU) based RNN, which aim to solve vanishing gradient problem caused by vanilla RNNs, proved their success on sequential data, and autoencoder with deep neural network layers showed success for noise reduction, in this research autoencoders with GRU layers were investigated to see if they are successful as PCA, which is used as a baseline in this research for noise reduction to increase the SNR.

Can a stacked autoencoder built upon Gated Recurrent Unit based Recurrent Neural Network layers (GRU-AE) perform better and have a higher signal-to-noise ratio when

compared to Principal Component Analysis for noise reduction of electroencephalography signals?

1.3 Research Objectives

The objective of this research is to investigate the effectiveness of the deep learning approach GRU-AE for noise reduction on EEG signals by conducting a literature review for deep learning techniques and noise reduction techniques for EEG data. To compare the performance of GRU-AEs against one of the traditional techniques PCA, signals will be reconstructed with both approaches and SNRs of reconstructed signals from GRU-AE and PCA will be calculated and compared with the Harrell-Davis test.

1.4 Research Methodologies

This research can be categorised by four group; by its type, its objective, its form and by its reasoning.

By type, this research is a secondary, also known as desk research, because it is a systematic review and a collation and expansion of an existing research and the data already exists.

By objective, it is quantitative since it is aimed to develop hypotheses pertaining to related phenomena and EEG signals are the numerical data and it allows the measurement of SNR to be compared by calculation of the Harrell-Davis test.

By form, this research is an example of empirical research because research hypothesis was defined and tested with a scientific method and the knowledge was gained by direct observation.

For the last category, by reasoning, it is deductive because it is a top-down approach; from a theory the hypotheses were built, tested and the results were observed then the confirmation was made.

1.5 Scope and Limitations

The scope of this research is the noise reduction on the EEG signals using GRU-AEs. Because of the required training time for GRU-AE and the size of the data, the main limitations of this research are time and available computational power. The research is limited with one dataset. The data used in this research was collected from a study (Ford, Palzes, Roach & Mathalon, 2013) and extensions of this study. EEG signals in the data are from 81 subjects; 49 of them diagnosed with schizophrenia and 32 of them are healthy control subjects. Since the aim of this study is reducing the noise on EEG signals, demographics of the subjects were not be analysed.

1.6 Document Outline

The remaining chapters of this research structured as follows:

Chapter 2 – Literature Review and Related Work

This chapter focuses on existing literature about Event Related Potentials, EEG, noise reduction techniques, related works with machine learning and deep learning on EEG data and autoencoders. Also, a table for summary of reviewed papers, gaps in the research and research question can be found in this chapter.

Chapter 3 – Design and Methodology

Research hypothesis is described in this chapter. Also, the data used in this research, architecture of the models, hyperparameters, strengths and limitations of the architecture are mentioned. Finally, technical and semantic evaluation metrics are described.

Chapter 4 – Results, Evaluation and Discussion

In this chapter, the findings from the experiment are described. Selected model's performance is evaluated, strengths and limitation of the selected model are detailed, and possible improvements are discussed.

Chapter 5 – Conclusion

This chapter gives an overview of the experiment which was carried out in this research with its results and further work is included.

2. LITERATURE REVIEW AND RELATED WORK

In this chapter, literature review about Event Related Potentials, EEG, noise reduction techniques, applications of deep learning techniques on EEG data, autoencoders for noise reduction on EEG are mentioned.

2.1 Event Related Potentials (ERPs)

Event Related Potentials (ERPs) are voltage changes induced in the brain in response to various cognitive, sensory and motor events (Friedman & Johnson, 2000). First known ERPs were recorded in 1935-1936 by Pauline and Hallowell Davis who is an American physiologist, otolaryngologist and researcher and it became popular in the middle 1980s (Luck, 2005). ERPs have been used for over 80 years to study brain's electrical activity following events of interest. (Thigpen, Kappenman & Keil, 2017) They represent neural activity evoked by an event and they can be used to investigate how the information is processed by the brain over time (Rugg, 2001). It is frequently used in general, experimental, clinical psychology and biomedical engineering. Amplitude, latency, and scalp distribution are the three measurable aspects of an ERP waveform (Johnson, 1992).

2.2 Electroencephalography (EEG)

EEG is a non-invasive electrophysiological method for measuring and recording the electrical activities in the brain. The difference between the EEG and ERP is that the EEG signals are spontaneous whereas ERPs are generated with an external stimulus.

Electrical activities in the brain can be expressed in time series waveforms. EEG waveforms commonly classified by their frequency, amplitude and location on the scalp where electrodes are placed for recording. For a healthy person, EEG amplitude lies between the range of 10-10000μV having following frequency components; *Delta* (0.1-4 *Hz*), *Theta* (4-8 *Hz*), *Alpha* (8-13 *Hz*), *Beta* (13-30 *Hz*), *Gamma* (30-100 *Hz*) (Kaushal, Singh & Jain, 2016). Delta waves represent the grey matter of the brain. It can be found in all sleep stages and it induces growth hormone. Theta waves are related to subconscious activities and can be observed in deep relaxation. They are linked to the production of growth hormone and serotonin. Alpha waves represent the white matter of the brain. Those waves can act as a bridge between conscious and subconscious mind.

They induce serotonin. Beta waves are related to behaviour and actions. They can be observed in conscious state and they are linked to the production of Cortisol. Lastly, Gamma waves are related to consciousness and perception and they induce serotonin and endorphins. (Kumar & Bhuvaneswari, 2012).

EEG signals can be obtained by placing electrodes on the subject's scalp. The 10-20 system is widely used for the placement of the electrodes. It is an internationally recognized system that standardized the electrode positions and provides reproducibility and comparability of results of the EEG signals analysis from different research (Jasper, 1958). In this system, scalp is divided into five parts; frontal (F), temporal (T), central (C), parietal (P), and occipital (O). In each of those parts, the electrodes in the right side of the brain are denoted by even numbers and the electrodes on the left are denoted by odd numbers (Sahu, Nagwani & Verma, 2016). The "10" and "20" indicate that the distances between contiguous electrodes are either 10% or 20% of the total front-back or right-left distance of the skull (Homan, Herman & Purdy,1987). The 10-20 electrode placement system can be seen in Figure 2.2-1.

Each electrode that captures the brain activity is called as a channel. Number of channels can vary based on the related research. This number can be up to 256 (Lau, Gwin & Ferris, 2012; Foresta, Morabito, Marino & Dattola,2019). In this research, EEG signals in the dataset were recorded by 64 channels.

EEG analysis is extensively used for medical purposes such as diagnosing, monitoring diseases and disorders about the nerves, also used for neuroscience, cognitive science, cognitive psychology, neurolinguistics and psychophysiological research (Jafarifarmand & Badamchizadeh, 2013).

EEG signals are low voltage signals, as it is mentioned before they contain many undesired noises which can be also called artefacts. Artefacts can be divided into two groups: external and biological. External artefacts generally caused by technical factors such as line interference and electrodes. Biological artefacts are mostly because ocular or muscular (Jafarifarmand & Badamchizadeh, 2013). Most common biological artefacts in the EEG signals are eye blinks, eye movement, arm movement, head

movement, jaw clenching and swallowing (Leite et al., 2018). If the noise in the EEG signal is not reduced properly, the results of the EEG analysis can be highly misleading.

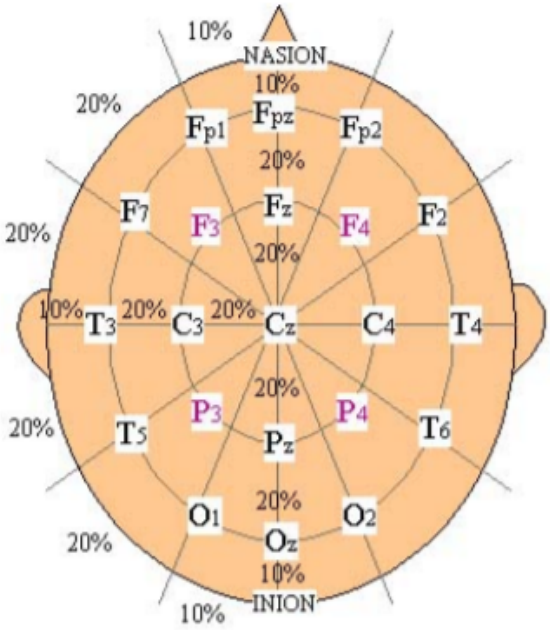

Figure 2.2-1 The 10-20 system (Kan & Lee, 2015)

Level of noise in the signals can be compared to the level of desired signal with the signal-to-noise ratio (SNR) (Kaushal et al., 2016). It gives a ratio of the signal power to the noise power present in a signal. Signal (S) can be calculated as the square root of the sum of the squared signals in the reading divided by the length of the reading. Noise (N) can be calculated as the square root of the sum of the squared noise in the reading divided by the length of the reading and SNR can be calculated by the common logarithm of the ratio of the signal and noise multiply by 20. Mathematical representation of the SNR is:

$$SNR = 20\ \log_{10}(\frac{S}{N}) \quad ;$$

$$N = \sqrt{\frac{\sum(noise)^2}{len(noise)}} \qquad S = \sqrt{\frac{\sum(signal)^2}{len(signal)}}$$

Where *signal* is the voltage amplitude readings of the signal, *noise* is the voltage amplitude readings of the noise and *len* is the length of readings. With noise reduction techniques, SNRs can be increased.

2.3 Traditional Noise Reduction Techniques

In this section, most common traditional noise reduction techniques such as Principal Component Analysis, Independent Component Analysis and Wavelet transformation and their applications on EEG data will be described.

2.3.1 Principal Component Analysis (PCA)

PCA, invented by Karl Pearson in 1901 (Pearson, 1901), is a method that extensively used in statistics, signal processing, and neural computing for feature extraction and denoising. It transforms the correlated values into uncorrelated values. First, it applies linear algebra computation on the covariance matrix of the data to produce set of eigenvectors and eigenvalues. Then linear combinations of the original data weighted by those eigenvectors to transform the attributes which are called *principal components*. Number of principal components is equal or less than the actual number of variables. Those components account for maximally explaining the variance in the data (M'ng & Mehralizadeh, 2016; Khatwani & Tiwari, 2013; Haufe, Dahne & Nikulin, 2014; Helal, Eldawlatly & Taher, 2017). In some applications, percentage of explained variance by the components is defined as a threshold, which is usually in the range of 80%-95% (Artoni, Delorme & Makeig, 2018). In this research 95% is selected for the explained variance (Hair, Anderson, Tatham & Black, 1995).

PCA has been applied directly for noise reduction (Artoni et. al, 2018). It is used for extracting ERPs (Bromm & Scharein, 1982), subsequent frequency domain analyses, identifying and removing artefacts (Lagerlund, Sharbrough & Busacker, 1997; Casarotto, Bianchi, Cerutti & Chiarenza, 2004; Ghandeharion & Erfanian, 2010). It is firstly used for removing the ocular artefacts which are blinks and eye movement from a multichannel EEG data (Scherg & Berg, 1991).

For signal processing, PCA is extensively used for epileptic seizure detection using EEG signals (Ahmad, Fairuz, Zakaria & Isa, 2008; Subasi & Gursoy, 2010; Kevric & Subasi, 2014; Xun, Jia & Zhang, 2016; Wang, Gong, Li & Qui, 2019).

Since PCA detects the coherent activity over data and removes the part of an EEG data that is spatially correlated over the scalp, it helps to increase the SNR (Kobayashi & Kuriki, 1999; Casarotto et. al, 2004).

2.3.2 Independent Component Analysis (ICA)

Another feature extraction and denoising technique is ICA. It was introduced by Herault and Jutten in 1986 (Herault & Jutten, 1986) and in the middle 1990s its mathematical formulation was presented (Comon, 1994). ICA is originally developed for blind source separation then it was generalized for feature extraction (Romero, Mananas, Clos, Gimenez & Barbanoj, 2003; Cao, Chua, Chong, Lee & Gu, 2003; Safieddine, Kachenoura, Albera, Birot, Karfoul, Pasnicu, Biraben, Wendling, Senhadji & Merlet, 2012). It decomposes the mixed input data into set of *independent components* (ICs) (James, Kobayashi & Lowe, 1999). It uses high-order statistics and maps nonorthogonal and its components are statistically independent whereas PCA uses second order spatio-temporal correlation information and finds orthogonal directions of the maximum variance and its components are uncorrelated (James et.al, 1999; Jung, Makeig, Humphries, Lee, McKeown, Iragui & Sejnowski, 2000; Cao et.al, 2003).

ICA decomposes the EEG recordings into a brain-related and artefact- related ICs. After that, noise-free signal can be reconstructed by extracting the artefact-related ICs from the EEG signal (Romero et. al, 2013; Radüntz, Scouten, Hochmuth & Meffert, 2017). It has been proven that ICA performs more successful when the EEG signal has more channels (Jung, Humphries, Lee, Makeig, McKeown, Iragui & Sejnowski, 1997; Ungureanu, Bigan, Strungaru & Lazarescu, 2004). ICA is widely used for noise reduction and showed that it can successfully identify and remove ocular and muscular artefacts especially for eye movements and blinking based artefacts from EEG recordings (Vigário, Särelä, Jousmäki, Hämäläinen & Oja, 2000; Jung et. al, 2000; Vorobyov & Cichocki, 2002; Iriarte, Urrestarazu, Valencia, Alegre, Malanda, Viteri & Artieda, 2003; James & Gibson, 2003; Delorme & Makeig, 2004; Joyce, Gorodnitsky & Kutas, 2004; Flexer, Bauer, Pripfl & Dorffner, 2005; Crespo-Garcia, Atienza & Cantero, 2008; Zhou & Gotman, 2008; Safieddine et.al,2012; Somers & Bertrand, 2016; Zou, Nathan & Jafari, 2016; Frølich & Dowding, 2018).

2.3.3 Wavelet Transformation

Wavelet transformation, also known as wavelet decomposition, which was formulated by Grossman and Morlet (1985), is a time-frequency analysis technique that transforms a time domain signal into different frequency components to provide an understanding about the characteristic of the signal (Kumar, Arumuganathan, Sivakumar & Vimal, 2008; Turnip & Pardede, 2017; Heydari & Shahbakhti, 2015; Maddirala & Shaik, 2016; Satapathy, Dehuri & Jagadev, 2016). It decomposes the signal into a set of functions called wavelet functions which fulfils the conditions such as zero mean amplitude, continuity and finite or near finite duration (Adeli, Zhou & Dadmehr, 2003) and has been frequently applied in signal processing for the feature extraction and denoising. Wavelet transformation can be divided into two categories; Continuous Wavelet Transform (CWT) and Discrete Wavelet Transform (DWT). In the CWT, the input signal is expressed as a "weighted integral of the continuous wavelet function" and in the DWT, it is expressed as a "weighted sum of series of wavelet functions" because wavelet functions are taken at discrete points (Adeli et al., 2003; Satapathy et al., 2016).

Wavelet transformations, especially DWT, which was found computationally faster than the CWT, has been used on EEG signals for epileptiform pattern detection (Indiradevi, Elias, Sathidevi, Dinesh Nayak & Radhakrishnan, 2008), epileptic seizure detection and characterization (Schiff, Aldroubi, Unser & Sato, 1994; Goelz, Jones & Bones, 2000; Alegre, Labarga, Gurtubay, Iriarte, Malanda & Artieda, 2003; Mormann, Fell, Axmacher, Weber, Lehnertz, Elger & Fernandez, 2005; Sharma, Pachori & Acharya, 2017; Wang et al., 2019), artefact removal (Zikov, Bibian, Dumont, Huzmezan & Ries, 2002; Rong-Yi & Zhong, 2005; Krishnaveni, Jayaraman, Anitha & Ramadoss, 2006; Aminghafari, Cheze & Poggi, 2006; Iyer & Zouridakis, 2007; Kumar et al., 2008; Akhtar, Mitsuhashi & James, 2012; Safieddine et. al, 2012; Jafarifarmand et al., 2013; Peng, Hu, Shi, Ratcliffe, Zhao, Qi & Gao, 2013; Mahajan & Morshed, 2015; Heydari & Shahbakhti, 2015; Turnip & Pardede, 2017).

2.4 Machine Learning and Deep Learning for EEG

As mentioned above, most common traditional noise reduction techniques have been used for denoising the EEG signals and they successfully increased the SNR. In addition

to those traditional techniques, machine learning and deep learning approaches are also used on EEG data for different purposes.

Machine learning and deep learning have important roles in our lives, range of its application areas are extremely wide. One of the developing areas is the signal processing, especially for EEG signals.

2.4.1 Supervised and Unsupervised Machine Learning

An American computer scientist Tom Mitchell defines machine learning as "A computer program is said to learn from experience E with respect to some class of tasks T and performance measure P, if its performance at tasks in T, as measured by P, improves with experience E." (Mitchell, 1997).

Machine learning can be divided into two broad groups; supervised learning and unsupervised learning. In supervised learning, data is labelled, each instance is associated with a provided target value. It learns to predict new examples' target values from a training set of examples of features and targets.

Supervised learning tasks can be grouped as regression, where targets are continuous values and classification, where targets are categories. Logistic regression, decision tree, Support Vector Machine (SVM), random forest and k-nearest neighbors (kNN) are some examples for the supervised learning algorithms.

In unsupervised learning, data is unlabelled, which means that data does not contain any target values. It learns to draw samples from a distribution, discover interesting structures in the data, denoise the data from some distribution and learns to cluster the data into related groups. Some of the popular unsupervised algorithms are; k-means clustering and hierarchical clustering. PCA and ICA can be also counted as an unsupervised learning algorithm. (Goodfellow, Bengio & Courville, 2016)

2.4.2 Deep Learning

Deep learning is a subfield of machine learning which is inspired by the biological neural networks of the brain (Goodfellow et al., 2016). It extracts low-level and high-level features of the data without any manual feature selections (Lauzon, 2012; Li, Lee, Jung, Youn & Camacho, 2019).

Neural Networks (NN) are the set of algorithms, inspired by the human brain. They consist of at least three layers; input layer, hidden layer and output layer. Input layers take the input data, hidden layers encode high-level features between input and output and output layers which capture the result of the model and outputs the predicted value. Each layer contains neurons, also referred to as units, which are connected with each other by weights. It is possible to have more than one hidden layer. Deep learning architectures are the architectures which contain at least two hidden layers. An example for a deep learning architecture with two hidden layers can be found in Figure 2.4.2-1. They can directly optimize their parameters and extract features by automatically updating its weights with backpropagation (Li et al., 2019; Craik, He & Contreras-Vidal, 2019).

Deep learning is extensively and successfully used for various research area. Some of those are; emotion recognition, seizure detection, natural language processing, computer vision. Most prevalent deep learning architectures Convolutional Neural Networks (CNNs), Recurrent Neural Networks (RNNs) and Autoencoders (AEs) will be examined for EEG data in this research.

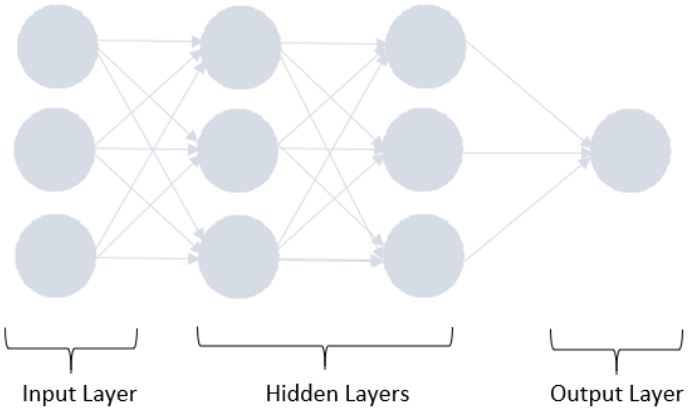

Figure 2.4.2-1 Deep learning architecture with two hidden layers

2.4.3 Applications of Deep Learning on EEG Data

2.4.3.1 Convolutional Neural Network (CNN)

CNN is a type of deep neural network architecture. The concept is rooted in a work by Hubel and Wiesel which is about primary visual cortex of cats and monkeys. It is noted that their visual cortex contains neurons that individually respond to small regions of the visual field (Hubel & Wiesel, 1968) which are similar to CNN's filters. (LeCun, Kavukcuoglu & Farabet, 2010). Inspired by Hubel and Wiesel, Fukushima designed the first CNN architecture which is called "Neocognitron" (Fukushima, 1980). In 1989, LeCun combined the CNN with backpropagation to learn hand-written digits (LeCun, 1989).

CNN consists of convolutional layers and pooling layers. Convolutional layers contain filters, sometimes referred to as convolutional kernels, feature detectors which are applied systematically on the input to produce subsamples of the input, called feature maps. Pooling layers are used for reducing the size of those feature maps. Generally maximum pooling is used to preserve the strong features (LeCun et al., 2010; Yao, Plested & Gedeon, 2018). CNN has proved its success on many tasks such as object recognition and detection, speech recognition, computer vision with image, video, sound and text.

Hence CNNs can directly extract features, no prior knowledge is required about the data and availability of large datasets for EEG signal is increased, CNN architectures are frequently used on EEG data for various tasks.

Mirowski, Madhavan, LeCun and Kuzniecky (2009) compared the performance of the CNN with logistic regression, and SVM for epileptic seizure detection. As a pre-processing, they used wavelet transforms for feature extraction, then they separately fed them into CNN and other models. They reported that CNN outperformed other models. Antoniades, Spyrou, Took and Sanei (2016) also compared different CNN architectures for epileptic seizure detection and reported that more than two convolutional layers do not improve the accuracy. Liang, Lu, Wang and Zhang (2016) applied CNN with SVM at the end of the architecture and compared it with random forest and they reported that

CNN architecture resulted with higher accuracy for epileptic seizure detection. Page, Shea and Mohsenin (2016) used CNN with maximum pooling layer connected to a softmax classifier for another epileptic seizure detection task. Different than the previous examples, Acharya, Oh, Hagiwara, Tan and Adeli (2018) increased the depth and used thirteen layered CNN with 5 convolutional layers with 5 maximum pooling layers and three fully connected layers. Ullah, Hussain, Qazi and Aboalsamh (2018) proposed an ensemble of pyramidal one-dimensional CNN models and connected them with a softmax classifier for epileptic seizure detection. Finally, for the epileptic seizure detection, Wei, Zhou, Chen, Zhang and Zhou (2018) and Emami, Kunii, Matsuo, Shinozaki, Kawai and Takahashi (2019) converted EEG signals into images to use as input for CNN.

For emotion recognition tasks, Yanagimoto and Sugimoto (2016) used CNN consists of 5 convolutional layers with one fully connected layer and a softmax layer. Qiao, Qing, Zhang, Xing and Xu (2017) used CNN consists of two convolutional layers following by a maximum pooling layer then a fully connected layer and output layer with a softmax classifier and Salama, El-Khoribi, Shoman and Shalaby (2018) used CNN which contains 2 convolutional layers, each of them following by a maximum pooling layer, and they connected them into fully connected layer with a softmax classifier. Finally, for the emotion recognition Yang, Han and Min (2019) applied multi-column structure consist of 5 CNNs and they used weighted sum for the final decision. They reported that their architecture outperformed existing models.

For motor imagery tasks, Sakhavi, Guan and Yan (2015) combined parallel CNNs with multilayer perceptron and reported that their architecture outperformed SVM and CNN architectures. Tang, Li and Sun (2017) used a CNN which consists of 2 convolutional layers with a fully connected layer and compared it with SVM, common spatial pattern with SVM, and autoregression and they concluded that CNN architecture can improve the classification performance. Wang, Cao, Zhang, Gong, Sun and Wang (2017) compared the CNN architectures with different activation functions such as Rectified Linear Unit (RELU), Scaled Exponential Linear Unit (SELU) and Exponential Linear Unit (ELU) and reported that CNN with SELU activation resulted with higher accuracy and finally for the motor imagery task, Abbas and Khan (2018) used Fast Fourier

Transform Energy Map for feature selection then applied a CNN and compared it with the existing 12 work and reported that their model can leverage the spatial and spectral information for more accurate classifications.

CNN architectures are also extensively used for mental workload tasks (Hajinoroozi, Mao, Jung, Lin & Huang, 2016; Jiao, Gao, Wang, Li & Xu, 2018; Zeng, Yang, Dai, Qin, Zhang & Kong, 2018) and abnormal EEG detection (Vrbancic & Podgorelec, 2018; Leeuwen, Sun, Tabaeizadeh, Struck & Westover, 2019).

2.4.3.2 Recurrent Neural Networks (RNN)

RNN is another type of a deep neural network. They are rooted based on a work by an American psychologist David Rumelhart (Rumelhart, 1986). They are successful with sequential data such as timeseries, audio, video and text, and they are widely used for machine translation, speech recognition, language modelling and text generation.

The network was inspired by the cyclical connectivity of neurons in the brain, it has loops, neurons in the hidden layers are recursive; which means that their output is connected back to itself, so output of a hidden layer are not only depend on the input at that timestep but also depend on the previous timesteps (Mirowski et al., 2009; Graves, 2012; Goodfellow et al., 2016). RNNs face vanishing gradient problems during training. To solve the vanishing gradient problems, Long Short Term Memory (LSTM) was introduced by Hochreiter and Schmidhuber in 1997. It is the special kind of RNN which can learn long-term dependencies (Michielli, Acharya & Molinari, 2019).

LSTMs can control which information to add to or remove from cell state by its gates. They contain 3 gates: input, output and forget gate. Forget gate controls which information to remove from the cell state, input gate controls which new information to add to the cell state and output gate controls which information to output based on the cell state (Yu, Si, Hu & Zhang, 2019). Diagram of LSTM can be seen in Figure 2.4.3.2-1.

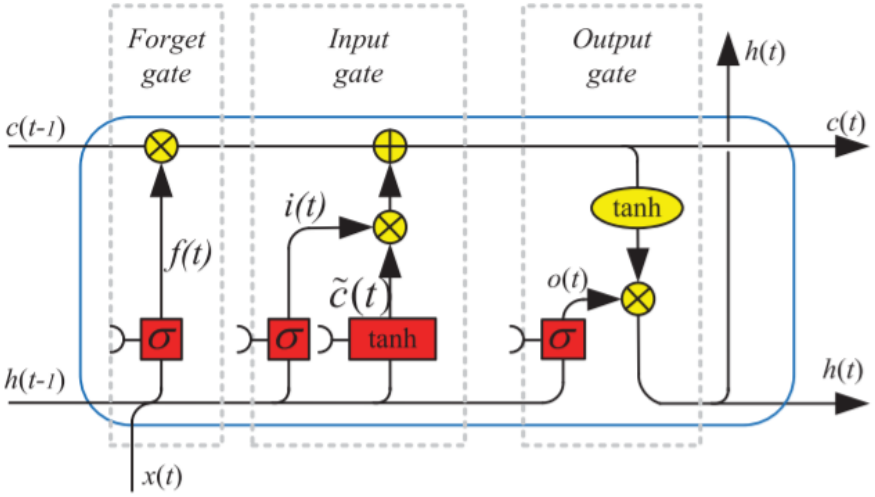

Figure 2.4.3.2-1 LSTM architecture (Yu et al., 2019)

As an alternative to the LSTM, Gated Recurrent Unit (GRU) was proposed in 2014 (Cho, Merriënboer, Gulcehre, Bougares, Schwenk & Bengio, 2014). The difference between LSTM and GRU is that GRU has 2 gates; update gate and reset gate. Update gate is the combination of forget gate and input gate from the LSTM. Update gate controls how much of the information from the previous timestep to keep and reset gates controls how much of the new information to pass to the next timestep. Diagram of a GRU can be seen in Figure 2.4.3.2-2.

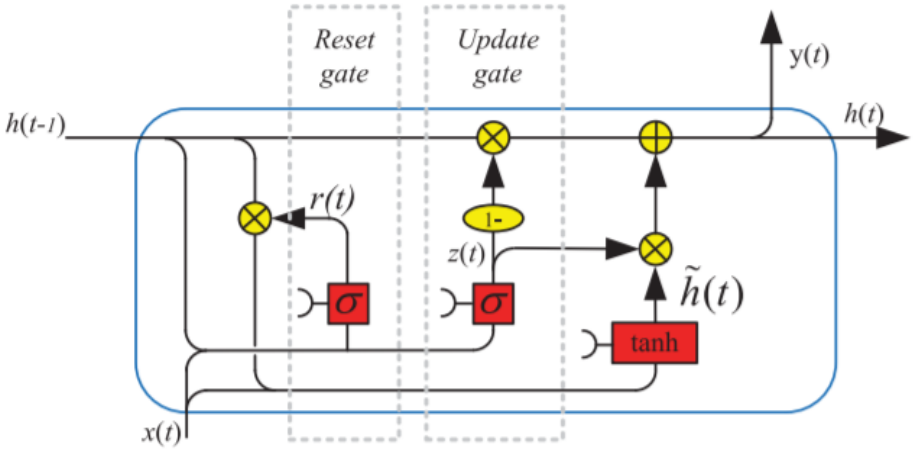

Figure 2.2.3.2-2 GRU architecture (Yu et al., 2019)

Since the EEG signals are also sequential, they have been extensively studied with different RNN architectures. LSTM architectures with various configurations are widely used for different tasks.

For seizure detection Vidyaratne, Glandon, Alam and Iftekharuddin (2016) used RNN, Ahmedt-Aristizabal, Fookes, Nguyen and Sridharan (2018) and Tsiouris, Pezoulas, Zervakis, Konitsiotis, Koutsouris and Fotiadis (2017) used LSTM followed by a fully connected layer. Tsiouris et al. (2017) also compared LSTM network's classification performance with decision tree and SVM and reported that LSTM outperformed other models. Finally, Hussein, Palangi, Ward and Wang (2019) used LSTM connected with a fully connected layer and compared the network with existing works' networks such as SVM, NN, decision tree, RNN and reported that their network outperformed those methods.

For emotion recognition, Soleymani, Asghari-Esfeden, Pantic and Fu (2014) used LSTM and compare it with multi-linear regression and support vector regressor and they reported that LSTM outperformed those methods and Alhagry, Fahmy and El-Khoribi (2017) also used LSTM and compared their method with 4 existing work and reported that their method achieved highest accuracy for the emotion classification. LSTM architectures were also successfully performed for motor imagery tasks (Wang et al., 2017; Wang, Jiang, Liu, Shang & Zhang, 2018; Luo, Zhou & Chao, 2018), lapse and confusion detection (Davidson, Jones & Peiris, 2007; Ni, Yuksel, Ni, Mandel & Xie, 2017) and sleep stage classification (Michielli et al., 2019).

RNN architectures have been also used with CNN architectures for hybrid models. Convolutional recurrent networks which are consist of convolutional layers and LSTM layers (Thodoroff, Pineau & Jim, 2016; Li, Song, Zhang, Yu, Hou & Hu, 2016; Li, Huang, Zhou & Zhong, 2017; Supratak, Dong, Wu & Guo, 2017; Bresch, Großekathöfer & Garcia-Molina, 2018; Hefron, Borghetti, Kabban, Christensen & Estepp, 2018; Kuanar, Athitsos, Pradhan, Mishra & Rao, 2018; Ma, Qiu, Du, Xing & He, 2018; Yang, Wu, Qiu, Wang & Chen, 2018) and convolutional layers with GRU layers (Golmohammadi, Ziyabari, Shah, Weltin, Campbell, Obeid & Picone, 2017; Roy, Kiral-

Kornek & Harrer, 2018; Affes, Mdhaffar, Triki, Jmaiel & Freisleben, 2019; Choi, Park, Kim, Cho & Kim, 2019) are the widely used hybrid models for CNN and RNN.

2.4.3.3 Autoencoders

Autoencoder (AE) is the NN that is used for unsupervised learning. AEs are similar to PCAs, they reduce the dimension by finding the important features of the input and they are widely used in denoising and feature extraction. AE's aim is to learn the compressed representation of the input. Example structure for an AE can be seen in Figure 2.4.3.3-1. They contain two main parts; "encoder" and "decoder". Encoder part takes the input and compresses it into reduced dimensional code. Then the decoder part reconstructs the input from that code (Lauzon, 2012; Xing et al., 2019), thus they reduce the dimension of the input without losing any important information. AEs try to minimize the loss function *L,* expressed by Goodfellow et al. (2016) as follows:

$$L(\boldsymbol{x}, g(f(\boldsymbol{x}))$$

There are many types of AE available such as sparse autoencoder, denoising autoencoders, variational autoencoders and stacked autoencoders. Stacked autoencoders are the AEs which are consist of multiple layers. Example structure for a stacked AE can be seen in Figure 2.4.3.3-2. The details of other types of AEs will be discussed in the next section.

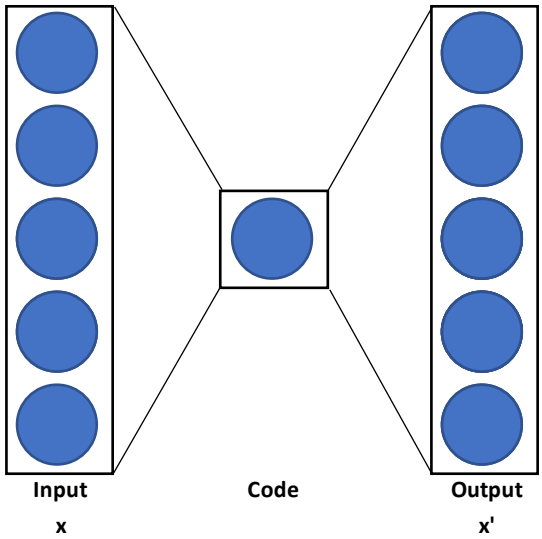

Figure 2.4.3.3-1 Autoencoder structure example

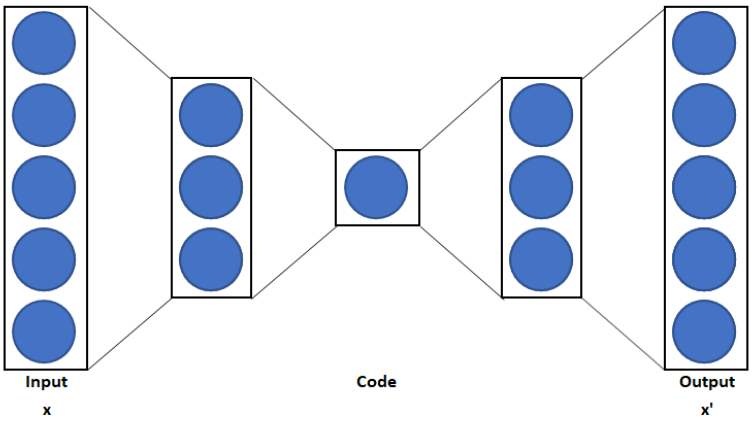

Figure 2.4.3.3-2 Stacked autoencoder structure example

EEG data has been used as an input for different types of AEs on various tasks. Helal et al. (2017) compared PCA and autoencoder for motor imagery tasks. They applied PCA then used linear discriminant analysis as a classifier for motor imagery task. Also, they used autoencoder with linear discriminant analysis classifier to compare the performances and they reported that autoencoder outperformed PCA. Jirayucharoensak, Pan-Ngum and Israsena (2014) used PCA for feature extraction, then they fed them into a stacked autoencoder which connected to a softmax classifier for an emotion recognition task. Supratak, Li and Guo (2014) used directly stacked autoencoders which connected to a softmax classifier for epileptic seizure detection. Yuan, Xun, Jia and Zhang (2017) converted EEG signals to spectrograms as inputs then fed them into stacked sparse denoising autoencoders for channel selection then for the detection of epileptic seizure they fed them into fully connected layer with a softmax classifier. Narejo, Pasero and Kulsoom (2016) used stacked sparse autoencoders connected with softmax classifiers for eye state classification and compared them with a deep belief network and reported that stacked sparse autoencoders outperformed deep belief network. Vařeka and Mautner (2017) used stacked autoencoder with a softmax classifier for P300 component detection and compared it with this task's state-of-the-art methods and they reported that stacked autoencoder resulted with higher accuracy. Tsinalis, Matthews and Guo (2016) first applied Morlet wavelet for feature extraction, then fed them into a stacked sparse autoencoder with softmax classifier for sleep stage classification.

Besides those examples, convolutional autoencoders (CAEs) which are autoencoders built upon convolutional layers also used on EEG data. Yao et al. (2018) converted EEG data into coloured images to use them as an input for a CAE for feature extraction and then connected them with fully connected layers for a classification task for alcoholism. Wen and Zhang (2018) were also use CAEs for feature extraction and then they fed them into different classifiers such as kNN, SVM and decision tree for epileptic seizure detection.

2.5 Autoencoders for Noise Reduction on EEG

As it mentioned above, there are various types of AE. In this section, sparse autoencoder, denoising autoencoders, variational autoencoders will be briefly described and examples of their applications for noise reduction on EEG data will be given.

2.5.1 Sparse Autoencoders

Sparse autoencoders are the autoencoders which have a sparsity penalty as training criteria. This penalty constrains the activation of the units in the hidden layers to be sparse, so the AE do not to entirely copy the input as an output, but it encourages the AE to learn the useful features. Sparse autoencoders try to minimize the loss function as follows (Goodfellow et al., 2016) ;

$$L(\boldsymbol{x}, g(f(\boldsymbol{x}))) + \Omega(\boldsymbol{h})$$

where $\boldsymbol{h}$ is the code layer, $\boldsymbol{h} = f(\boldsymbol{x})$ and $g(\boldsymbol{h})$ is the decoder output.

Sparse autoencoders have been used for noise reduction of EEG data (Lin, Ye, Huang, Li, Zhang, Xue & Chen, 2016; Yang, Duan & Zhang, 2016; Hosseini, Soltanian-Zadeh, Elisevich & Pompili, 2017; Yang, Duan, Fan, Hu & Wang, 2018). Yang et al. (2016) used sparse autoencoders for removing the electrooculogram artefacts from the EEG signal and they found out that noise reduction with spare autoencoder is time saving than ICA and it requires less channels for the removal. Lin et al. (2016) used stacked sparse autoencoder to reduce the noise then used softmax classifier for epileptic seizure

detection. Hosseini et al. (2017) first applied PCA and ICA on the EEG data, then they used stacked sparse autoencoder with a softmax classifier to detect epileptic seizure. Yang et al. (2018) used sparse autoencoders to remove ocular artefacts and reported that sparse autoencoders outperformed the traditional noise reduction techniques.

2.5.2 Denoising Autoencoders

Another type of AEs is the denoising autoencoder (Vincent, Larochelle, Bengio & Manzagol, 2008). The difference between denoising autoencoders and other autoencoders is that denoising autoencoders first corrupt the input $\boldsymbol{x}$ into $\tilde{\boldsymbol{x}}$ by some form of noise such as binary noise or Gaussian noise. Corruption by binary noise can be implemented by choosing randomly fixed number of input and force their value to be zero. Corruption by Gaussian noise can be implemented by adding a number of generated Gaussian random value into the data (Dong, Liao, Liu & Kuang, 2018). After corruption of the input, they stochastically learn to reconstruct the corrupted inputs into original input. The loss function for the denoising autoencoder is shown below (Goodfellow et al., 2016) ;

$$L(\boldsymbol{x}, g(f(\tilde{\boldsymbol{x}})))$$

Xu and Plataniotis (2016) used stacked denoising autoencoders for noise reduction then connected them with a softmax classifier for emotion recognition. Yin and Zhang (2017) used stacked denoising autoencoder for noise reduction then used multilayer perceptron classifier for mental workload task.

Denoising autoencoders can be used with a sparsity penalty thus they become denoising sparse autoencoders (Luo & Wan, 2013). Qiu, Zhou, Yu and Du (2018) used denoising sparse autoencoder, they both introduce sparsity penalty and corrupted the input. They reconstructed the EEG signals then fed them into a denoising sparse autoencoder with a softmax classifier for an epileptic seizure detection. Leite et al. (2018) used denoising sparse autoencoders which are consist of convolutional layers as a noise reduction technique.

2.5.3 Variational Autoencoders

Variational autoencoders are the generative models, which can generate samples that are not available in the input. They draw a sample $\boldsymbol{z}$ from the code distribution $p_{model}(\boldsymbol{z})$ and run it through a differentiable generator network $g(z)$ then $\boldsymbol{x}$ is sampled from a distribution $p_{model}(\boldsymbol{x};\ g(\boldsymbol{z})) = p_{model}(\boldsymbol{x} \mid \boldsymbol{z})$ (Goodfellow et al., 2016; Dong et al., 2018).

Wang, Abdelfattah, Moustafa and Hu (2018) used stacked variational autoencoder to extract features to fed into a Gaussian mixture-hidden Markov model for classification task. Aznan, Atapour-Abarghouei, Bonner, Connolly, Al Moubayed and Breckon (2019) used variational autoencoder built upon convolutional layers to generate synthetic EEG data to train a steady state visual evoked potential classifier. Bi, Zhang and Lian (2019) firstly used ICA and Kalman smoother for noise reduction of EEG before applying it directly into a variational autoencoder. After feature extraction with the autoencoder, they fed its output into SVM for a classification task. Dai, Zheng, Na, Wang and Zhang (2019) converted EEG data into image and fed them into a deep CNN for feature extraction. Then they used the output of the CNN as input to stacked variational autoencoder with a classifier for motor imagery task. They also compared the model with CNN, CNN followed by a stacked autoencoder and reported that CNN followed by a stacked variational autoencoder outperformed other models.

2.6 Summary of Literature Review

2.6.1 Table with Summary of Reviewed Papers

Reviewed papers about applications of deep learning on EEG data are summarised on the Table 2.6.1-1. As it can be seen from the table various types of deep neural networks have been used on EEG data for both supervised and unsupervised learning. Some investigations worked with a single channel EEG data and others worked with multi-channel EEG data which vary from 3 channels to 128 channels. For the classification tasks, it is reported that deep learning architectures such as CNNs, RNNs and AEs outperformed the classical supervised learning techniques such as decision trees and SVM. For the noise reduction, it is also reported that models trained with deep learning

architectures performed as successfully as or better than the traditional noise reduction techniques PCA, ICA and wavelet transformations.

2.6.2 Gaps in the literature

Deep learning architectures have been widely used for noise reduction, feature extraction or feature selection since the computational power is developed and availability of large EEG dataset is increased.

Hence the EEG signals are timeseries data, autoencoders built upon LSTM based RNN layers are constantly used directly for noise reduction and also for classification tasks with fully connected layers because they do not make any assumptions, they extract features without the need of any prior knowledge about the data and without identifying the artefacts manually and they easily overcome vanishing gradient problem. Although GRUs have simpler structure than LSTMs and they require less time for training, not much work done with GRU.

2.6.3 Research questions

"Can a stacked autoencoder built upon Gated Recurrent Unit based Recurrent Neural Network layers perform better and have a higher signal-to-noise ratio when compared to Principal Component Analysis for noise reduction of electroencephalography signals?"

Papers	Number of Channels	Application of Deep Learning	Copmarison Against Classical Methods
Helal et al. (2017)	22	AE	Yes
Wen & Zhang (2018)	23	CAE	No
Yao et al. (2018)	64	CAE	No
Abbas & Khan (2018), Wei et al. (2018)	22	CNN	Yes
Acharya et al. (2016), Ullah et al. (2018)	1	CNN	Yes
Antoniades et al. (2016)	12	CNN	No
Emami et al. (2018)	19	CNN	No
Hajinoroozi et al. (2016)	30	CNN	Yes
Jiao et al. (2018)	21	CNN	Yes
Liang et al. (2016), Yanagimoto & Sungimoto (2016)	24	CNN	Yes
Mirowski et al.(2009)	15	CNN	Yes
Page et al. (2016)	18	CNN	Yes
Qiao et al. (2017)	32	CNN	No
Sakhavi et al. (2015), Vrbancic et al. (2018)	8	CNN	Yes
Salama et al. (2018) , Yang et al. (2019)	32	CNN	Yes
Tang et al. (2017)	28	CNN	Yes
Zeng et al. (2018)	16	CNN	Yes
Affes et al. (2019), Choi et al. (2019)	23	CNN + GRU	No
Roy et al. (2018)	4	CNN + GRU	No
Golmohammadi et al. (2017)	1	CNN + GRU, CNN + LSTM	No
Bresch et al. (2018), Supratak et al. (2017)	1	CNN + LSTM	No
Hefron et al. (2018)	128	CNN + LSTM	No
Kuanar et al. (2018)	64	CNN + LSTM	Yes
Li et al. (2016), Li et al. (2017), Yang et al. (2018)	32	CNN + LSTM	Yes
Ma et al. (2018)	64	CNN + LSTM	No
Thodoroff et al. (2016)	3	CNN + LSTM	Yes
Wang et al. (2017)	3	CNN, LSTM	Yes
Leite et al. (2018)	19	Denoising Sparse AE	Yes
Qiu et al. (2018)	100	Denoising Sparse AE	Yes
Ahmedt-Aristizabal et al. (2018)	1	LSTM	No
Alhagry et al. (2017)	32	LSTM	Yes
Davidson et al. (2017)	16	LSTM	No
Hussein et al. (2019), Michielli et al. (2019), Ni et al. (2017)	1	LSTM	Yes
Soleymani et al. (2014)	14	LSTM	Yes
Tsiouris et al. (2017)	18	LSTM	Yes
Wang et al. (2018)	22	LSTM	No
Luo et al. (2018)	22	LSTM, GRU	Yes
Vidyaratne et al. (2016)	18	RNN	Yes
Yang et al. (2016)	3	Sparse AE	Yes
Yang et al. (2018)	32	Sparse AE	Yes
Jirayucharoensak et al. (2014)	32	Stacked AE	Yes
Supratak et al. (2014)	23	Stacked AE	No
Xing et al. (2019)	32	Stacked AE + LSTM	Yes
Xu et al. (2016)	32	Stacked Denoising AE	Yes
Yin et al. (2017)	11	Stacked Denoising AE	Yes
Hosseini et al. (2017)	15	Stacked Sparse AE	Yes
Lin et al. (2016)	128	Stacked Sparse AE	Yes
Narejo et al. (2016)	14	Stacked Sparse AE	No
Tsinalis et al. (2016)	1	Stacked Sparse AE	Yes
Yuan et al. (2017)	23	Stacked Sparse AE	Yes
Dai et al. (2019)	5	Stacked Variational AE	No
Wang et al. (2018)	52	Stacked Variational AE	No
Bi et al. (2019)	16	Variational AE	Yes
Aznan et al. (2019)	1	Variational AE with Convolutional Layers	No

Table 2.6.1-1 Summary of Reviewed Papers

3. DESIGN AND METHODOLOGY

In this chapter, the null hypothesis (H_0) and the alternate hypothesis (H_1) are described. Data understanding, data preparation, architecture of the models, hyperparameters, strengths and limitations of the architecture, technical and semantic evaluation metrics are also described in order to reject or accept the null hypothesis.

3.1 Hypothesis

$(\boldsymbol{H_1})$: If a stacked autoencoder built upon Gated Recurrent Unit based Recurrent Neural Network layers is used for noise reduction of electroencephalography signals, the signal-to-noise ratio can be increased when compared to Principal Component Analysis.

(H_0) : If a stacked autoencoder built upon Gated Recurrent Unit based Recurrent Neural Network layers is used for noise reduction of electroencephalography signals, the signal-to-noise ratio cannot be increased when compared to Principal Component Analysis.

3.2 Data

3.2.1 Data Understanding

The data used in this research is originally from a work by Ford et al. (2013) which can be found on Kaggle[1]. It contains EEG signals for 81 subjects; 49 of them diagnosed with schizophrenia and 32 of them are healthy control subjects, in separate 81 files. Each file has signals that were recorded by 64 electrodes (channels) which were placed on each subjects' scalps with 10-20 system. Each subject was recorded under three different conditions;

For condition 1 (Button Tone), in every 1-2 seconds subject pressed a button to deliver 1000 Hz, 80 dB sound pressure level, tone with no delay between pressing a button and tone onset. For condition 2 (Play Tone) subject passively listened to the tones that were generated for condition 1. For condition 3 (Button Alone) similar to condition 1, subject

[1] https://www.kaggle.com/broach/button-tone-sz

pressed a button but without a tone generated. Each condition has approximately 100 trials and each trial have a record for 700ms. The stimuli for each trial starts at 100ms, which indicates that first 100ms are considered as noise and the rest 600ms considered as signal combined with signal noise. An example of a signal from one channel and one trial can be seen from figure 3.2.1-1.

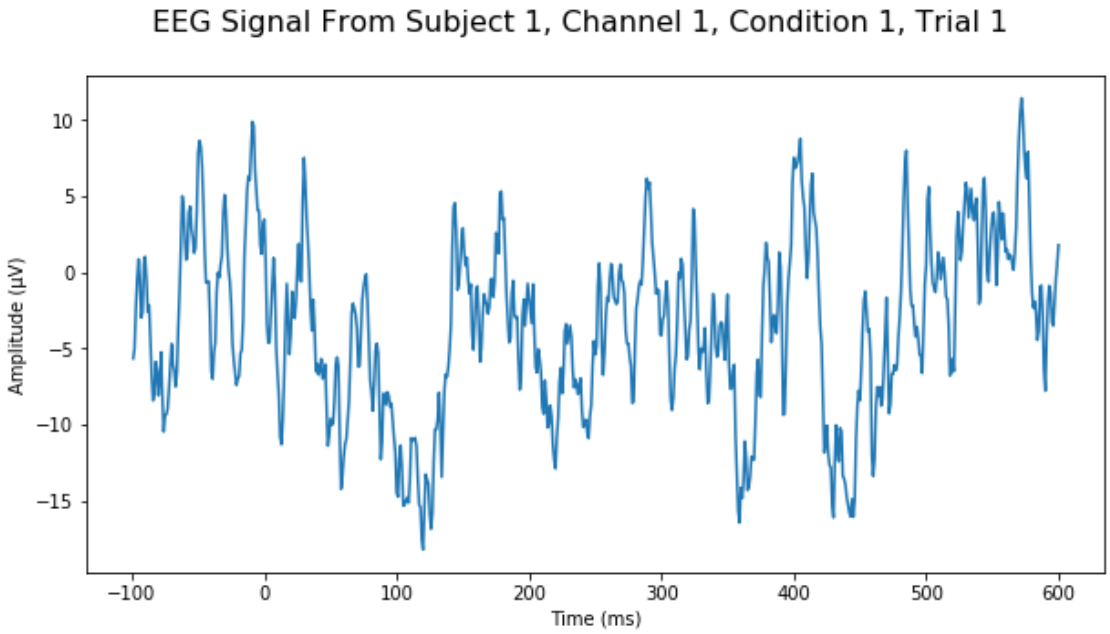

Figure 3.2.1-1 Example of an EEG signal

3.2.2 Data Preparation

As a data preparation step, firstly 81 files were combined into one list and subject 46 was removed because it does not have data for condition 3. Then the list was divided into 3 separate lists by each condition.

Hence EEG signals are sequences, for training and test splitting, data did not directly split randomly. Firstly, for each subject, each condition's trials were divided into 3 parts. Then randomly 70% of each part was selected for the train set and 30% for the test set. This split was applied for each condition for all subjects which resulted with 3 train sets and 3 test sets for each condition for multiple people (across subject).

For GRU-AE, input was reshaped as 3-dimensional array as (samples, timesteps, features). For sample, number of observations for each subject's each condition's each trial was considered, 700ms was taken into account as timesteps and 64 channels were considered as features. With all the data from 80 subjects, train and test sets became;

- For condition 1: train_C1 (5336, 700, 64), test_C1 (2402, 700, 64).
- For condition 2: train_C2 (5189, 700, 64), test_C2 (2355, 700, 64).
- For condition 3: train_C3 (5319, 700, 64), test_C3 (2395, 700, 64).

For the last step of data preparation, data was standardized with StandardScaler so the mean of the distribution became zero and the standard deviation became one.

3.3 Modelling

In this section design of the proposed architecture and its hyperparameters will be described.

3.3.1 GRU-AE Design

For the experiment, autoencoder built upon GRU based RNN layers is purposed as GRU-AE. Three main architectures were designed with different number of layers, and they were manipulated by different number of neurons. As a result, totally 9 models were designed, 3 for each main architecture which are;

- Architecture 1: AE with one GRU layer in the middle. For this architecture three models were designed where S is 45, 35 and 25.

- Architecture 2: AE with one GRU layer for the encoder part and one GRU layer for the decoder part. For this architecture three models were designed too. x_1 and S for those models are 19 and 45, 29 and 35, 39 and 25 respectively.

- Architecture 3: AE with two GRU layers for encoder and two GRU layers for decoder part. Three models were also designed for this architecture. x_1, x_2 and S for those models are 58, 55 and 45, 55, 45 and 35 and for the last model 51, 38 and 25 respectively.

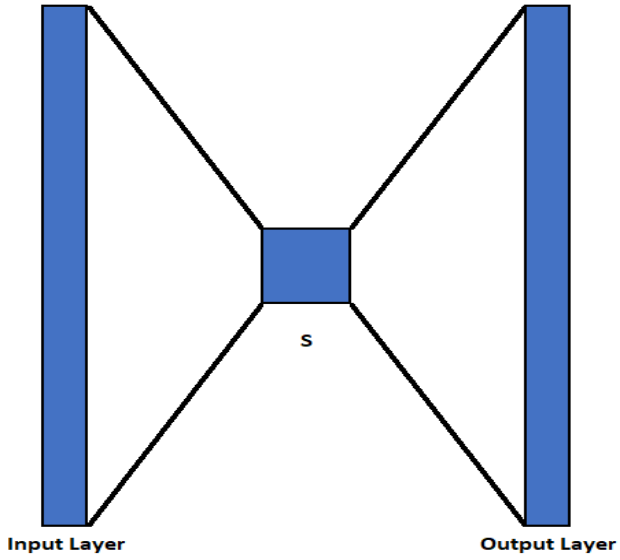

Figure 3.3.1-1 Architecture 1

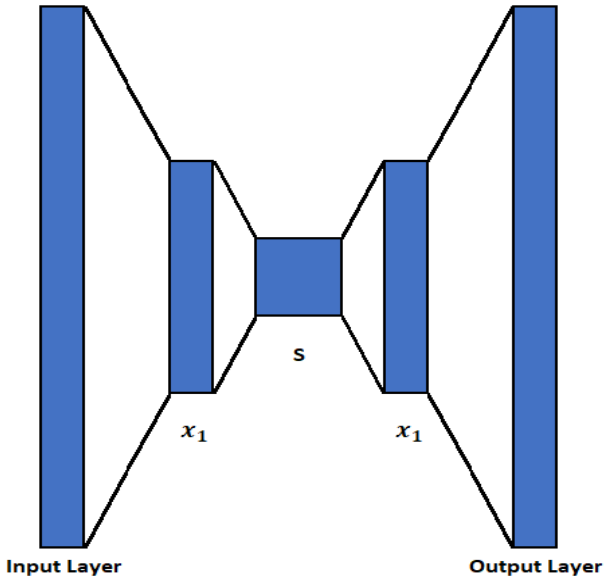

Figure 3.3.1-2 Architecture 2

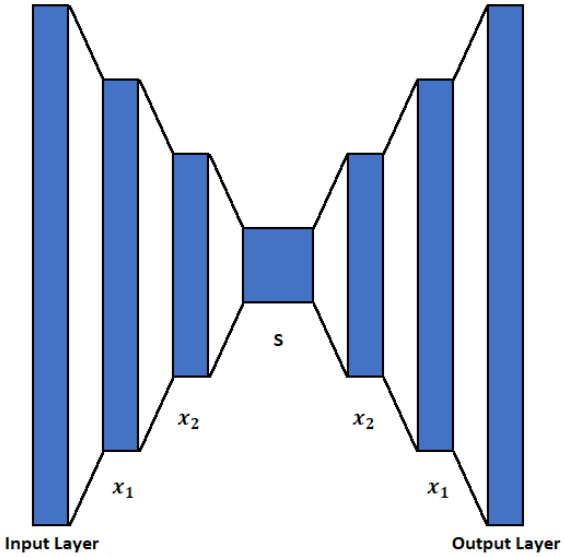

Figure 3.3.1-3 Architecture 3

3.3.2 Hyperparameters

It is important to select the right hyperparameters for an effective model. Hyperparameters for the GRU-AE are;

- ***Activation function :*** Activation functions determine the output of hidden neurons based on its input. They can be linear and non-linear. The default activation function for the GRU layer in Keras is hyperbolic tangent activation function (tanh). Since the EEG inputs are continuous signals, and the task is to reconstruct the EEG signals, outputs should not be limited in a range, they can be any real value. To have continuous real valued outputs, linear activation function is selected.
- ***Number of epochs :*** Number of epochs defines the number of times that the whole training set is passed forward and backward through the learning algorithm. To prevent overfitting, early stopping technique is applied. It will be trained till the validation error has failed to decrease for a set number of training iterations (model patience = 10).
- ***Batch size :*** Batch size is the number of training examples to be passed through the learning algorithm for each epoch. 512 is selected for the batch size.

- ***Optimizer :*** Optimizers help to reduce the error over time. Since they require little memory space and make the model converge faster than the other optimizers, Adam optimizer is selected.
- ***Dropout rate :*** Dropout is a regularization strategy that tries to prevent overfitting. The dropout rate is selected 0.25
- ***Loss function :*** Loss function is used to evaluate how well the learning algorithm models the given data. Reconstruction of timeseries EEG data with autoencoders can be treated as a regression problem. Mean Squared Error (MSE) is selected since it is commonly used for regression.

3.4 Evaluation of the Architecture

3.4.1 SNR

SNRs can be calculated with the following formula:

$$SNR = 20\ \log_{10}(\frac{S}{N})$$

$$N = \sqrt{\frac{\sum(noise)^2}{len(noise)}} \qquad S = \sqrt{\frac{\sum(signal)^2}{len(signal)}}$$

where *signal* is the voltage amplitude readings of the signal, *noise* is the voltage amplitude readings of the noise and *len* is the length of readings.

Since we know that the stimuli for each trial starts at 100ms, signal (S) and noise (N) can be easily calculated and eventually SNR can be calculated by the common logarithm of the ratio of the signal and noise multiply by 20.

For the comparison;

- SNR of the test data before the reconstruction,
- SNR of the PCA reconstructed test data,
- SNR of the GRU-AE reconstructed test data will be calculated for each condition.

3.4.2 Hypothesis Testing

To see whether the GRU-AE have significantly higher SNR than the PCA, firstly three training sets for each condition are fed into train 9 different GRU-AE models. Then three test sets for each condition are fed into both PCA and trained GRU-AEs to reconstruct the signals. After the reconstructions, reconstructed signals and raw signals (original signals from the test set) are plotted to see how accurate the signals are. SNRs for raw and reconstructed signals for each condition will be calculated. SNRs will be calculated for all trials by averaging 64 channels' SNRs (trial-wise).

Because of the nature of the brain signals, distributions of the SNRs generally overlap, and the difference cannot be seen when applying some of the statistical tests such as t-tests. Since it is a distribution-free approach, Harrell-Davis test will be conducted (Harrell & Davis, 1982).

Harrell-Davis decile values for the SNR distributions will be calculated for 9 deciles, then Harrell-Davis decile value differences between raw signals and PCA reconstructed signals (PCA_SNRs), and Harrell-Davis decile differences between raw signals and GRU-AE reconstructed signals (GRU_SNRs) will be calculated. To statistically show the performance of the model, mean difference of the GRU_SNRs and the PCA_SNRs will be compared.

Positive mean difference values will indicate that GRU-AE reconstructed signals have higher SNR when compared to PCA and it will show that there is an evidence to support to reject the null hypothesis and accepting the alternate hypothesis which indicates the GRU-AEs performed better than the PCA. Also, if majority of the decile values (5 or more deciles) are positive, it will also indicate that GRU-AE reconstructed signals have higher SNR than the PCA reconstructed signals.

Those evaluation steps will be conducted for 9 different GRU-AE models and each of them will be compared with PCA. The best model will be selected based on the mean Harrell-Davis decile value differences.

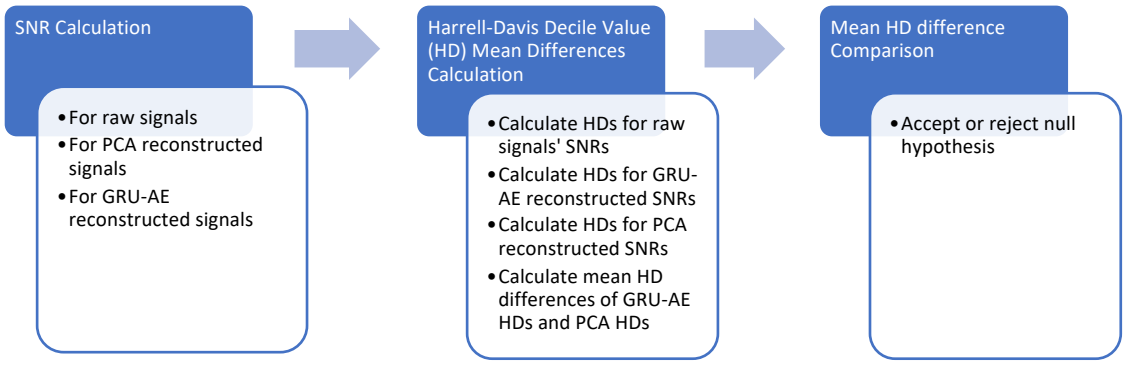

Figure 3.4.2-1 Evaluation summary

3.5 Summary

To see whether a stacked autoencoder built upon GRU based RNN layers increases the SNR when compared to PCA for noise reduction of EEG signals, 9 different GRU-AEs were designed with different number of hidden layers and neurons. For each condition, with 80 subjects, test signals were reconstructed with PCA. For the GRU-AEs, 9 models were trained separately with the training sets and tested with the test signals for each condition to reconstruct the signals.

For hypothesis testing, for each condition SNRs of the raw test signals and reconstructed signals will be calculated. Then Harrell-Davis decile values will be calculated for those SNR distributions and difference between raw test signals and reconstructed signals' SNR distributions will be calculated and examined. Positive mean difference decile values will indicate GRU-AEs perform better than the PCA.

3.5.1 Strengths of Design

- **Training time:** GRUs have simpler structure than LSTMs and they require less time for training.

- **Generally applicable:** Proposed models can be applied for other timeseries data for reconstruction.

- **Evaluation metric**: Because of the nature of the brain signals, distributions of the SNRs generally overlap, and the difference cannot be seen when applying other tests. A distribution-free metric Harrell-Davis will be used.

- **No prior knowledge required:** GRU-AEs can extract features without the need of any prior knowledge about the data and without identifying the artefacts manually.

- **Handling Vanishing Gradient :** Unlike vanilla RNNs, GRU based RNNs easily overcome vanishing gradient problem.

3.5.2 Limitations of Design

- **Training time:** Training deeper models with Architecture 3 requires more training time than Architecture 1, 2 and other deep learning architectures such as Convolutional autoencoders.

- **Using only one data**: Since the whole training set divided into 3 conditions, each set resulted with lower sample sizes.

- **Trial-wise:** Channel-wise analysis cannot be done since the SNRs are calculated by averaging the channels.

4. RESULTS, EVALUATION AND DISCUSSION

In this chapter, the results from the experiment are described and evaluated, strengths and limitation of the selected model are detailed, and possible improvements are discussed.

4.1 Results

For the experiment, raw test signals were fed into PCA for reconstruction. Also, 9 different GRU-AEs were designed with different number of hidden layers and neurons. Number of layer and neurons for each model can be seen in Table 4.1-1.

Architecture 1	(64,45,64) (64,35,64) (64,25,64)
Architecture 2	(64,45,19,45,64) (64,35,29,35,64) (64,39,25,39,64)
Architecture 3	(64,58,50,45,50,58,64) (64,55,45,35,45,55,64) (64,51,38,25,38,51,64)

Table 4.1-1 Architecture Structures

For the selected number of neurons, the models were trained with 3 train sets for each condition separately. Changes in the training and validation loss can be seen in Appendix A. After training, test signals were reconstructed with 3 models for Architecture 1. To see the reconstruction capacity of the GRU-AEs and PCA, raw signals were plotted against the reconstructed signals for each condition.

4.1.1 Architecture 1 Results

Plots for the first model of Architecture 1 (64,45,64) is displayed in the following figures (for randomly selected trial and channel). Plots from other models can be found in Appendix B.

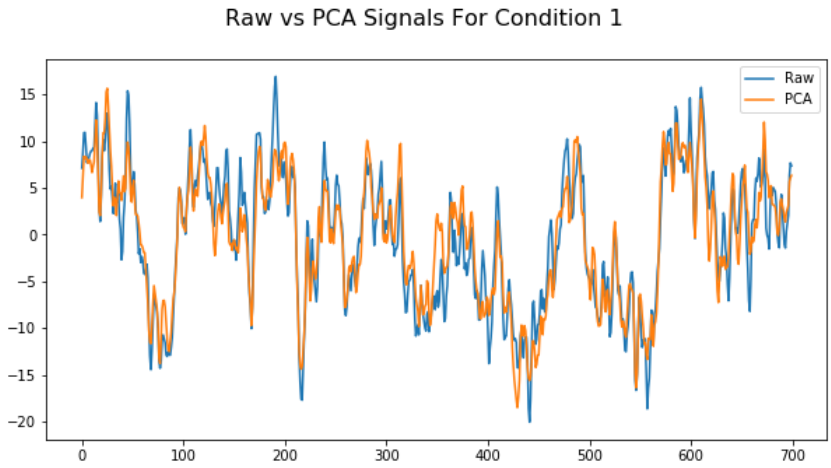

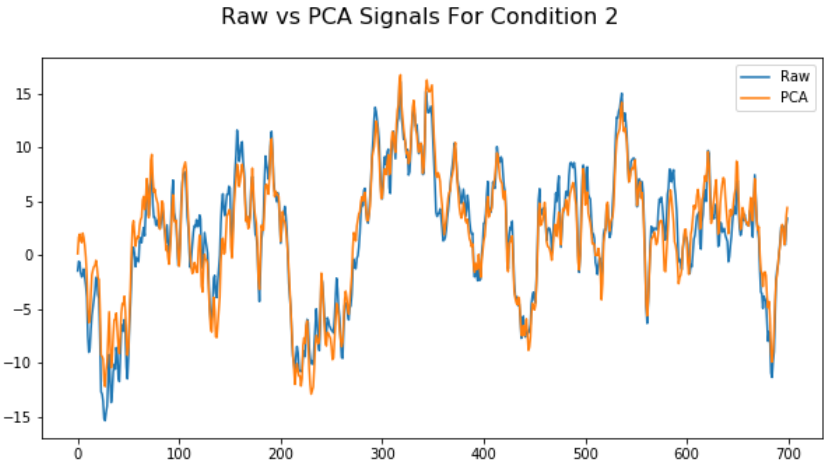

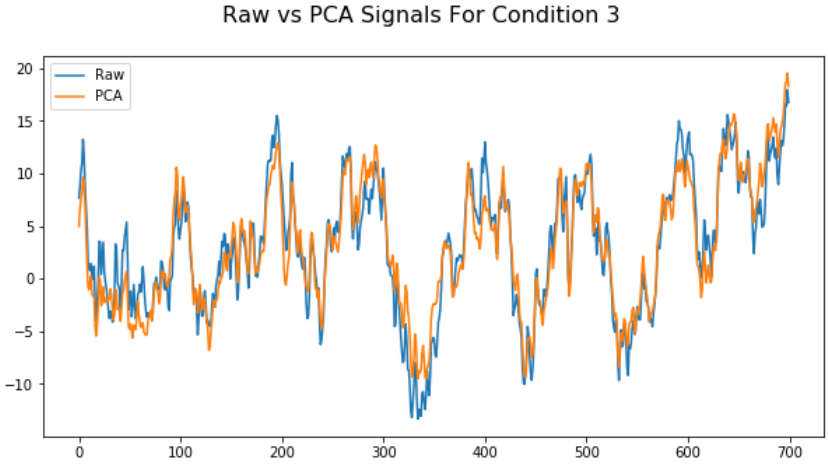

Figure 4.1.1-1 Raw vs PCA reconstructed signal for each condition

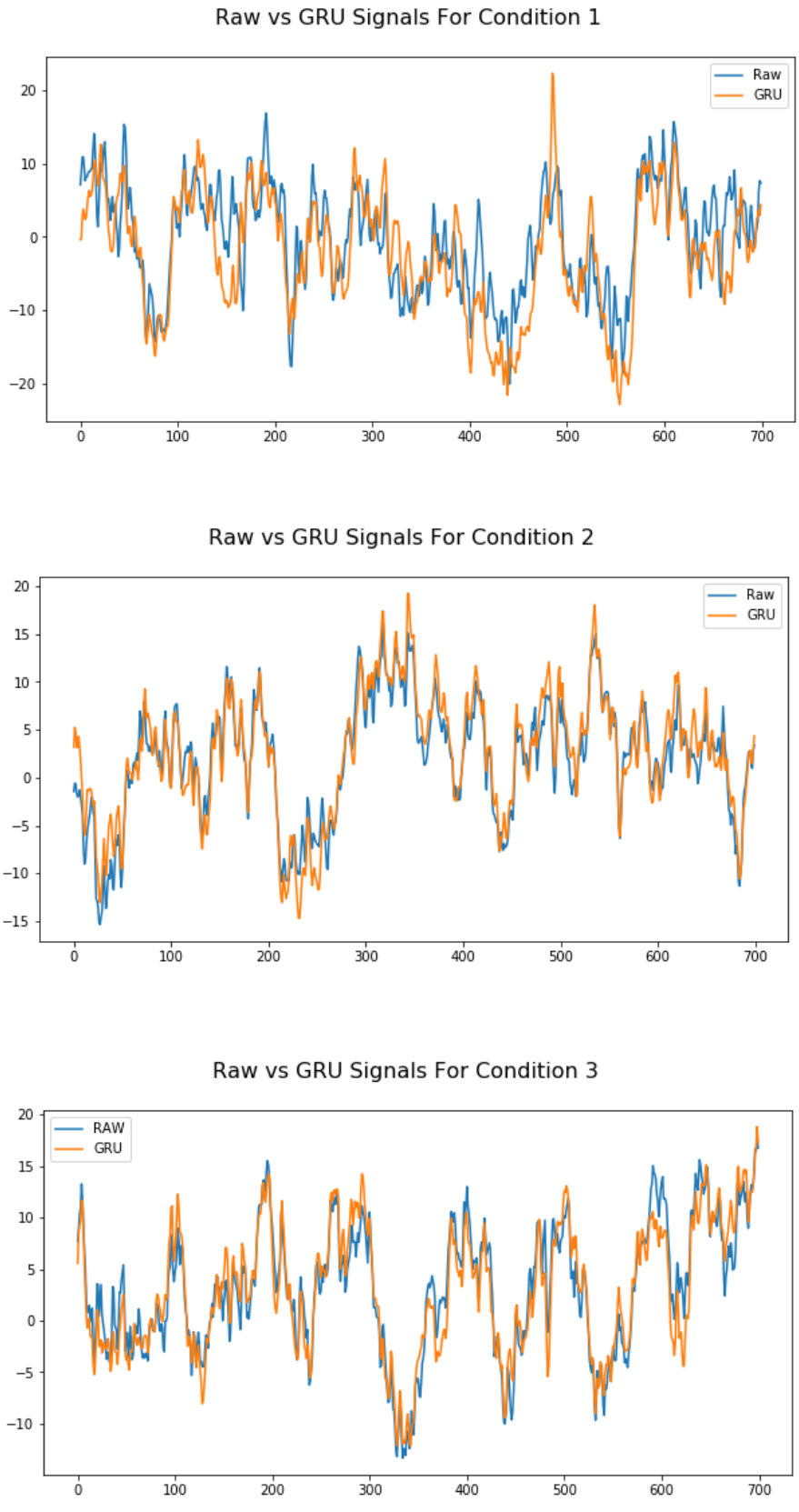

Figure 4.1.1-2 Raw vs GRU_AE reconstructed signal for each condition

4.1.2 Architecture 2 Results

To make the GRU-AE deep, one more layer was added to the encoder and the decoder part. Plots for the first model of Architecture 2 (64,45,19,45,64) is displayed in the Figure 4.1.2-1 and Figure 4.1.2-2 and others can be found in Appendix C.

4.1.3 Architecture 3 Results

To make the GRU-AE deeper, another layer was added to the encoder and the decoder part. Plots for the first model of Architecture 3 (64,58,50,45,50,58,64) is displayed in the Figure 4.1.3-1 and Figure 4.1.3-2 and others can be found in Appendix D.

From the plots, it can be seen that both PCA reconstructed signals and GRU-AE reconstructed signals are similar to raw signals.

After inspecting the reconstruction capacity visually, for testing the hypothesis, SNRs for raw signals, PCA reconstructed signals and GRU-AE reconstructed signals were calculated and Harrell-Davis decile values were calculated for each SNR distribution.

SNR distributions for each model was plotted and based on the mean difference decile values, best model was selected.

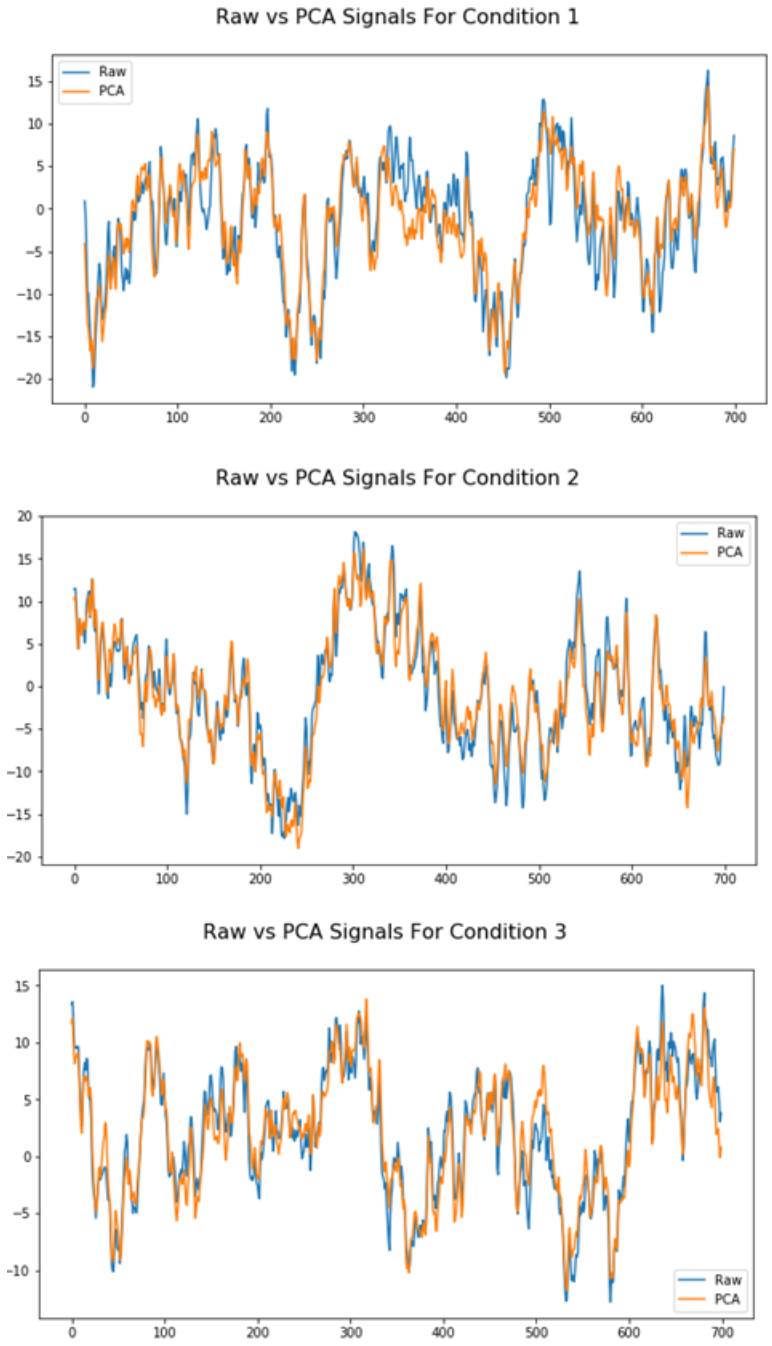

Figure 4.1.2-1 Raw vs PCA reconstructed signal for each condition

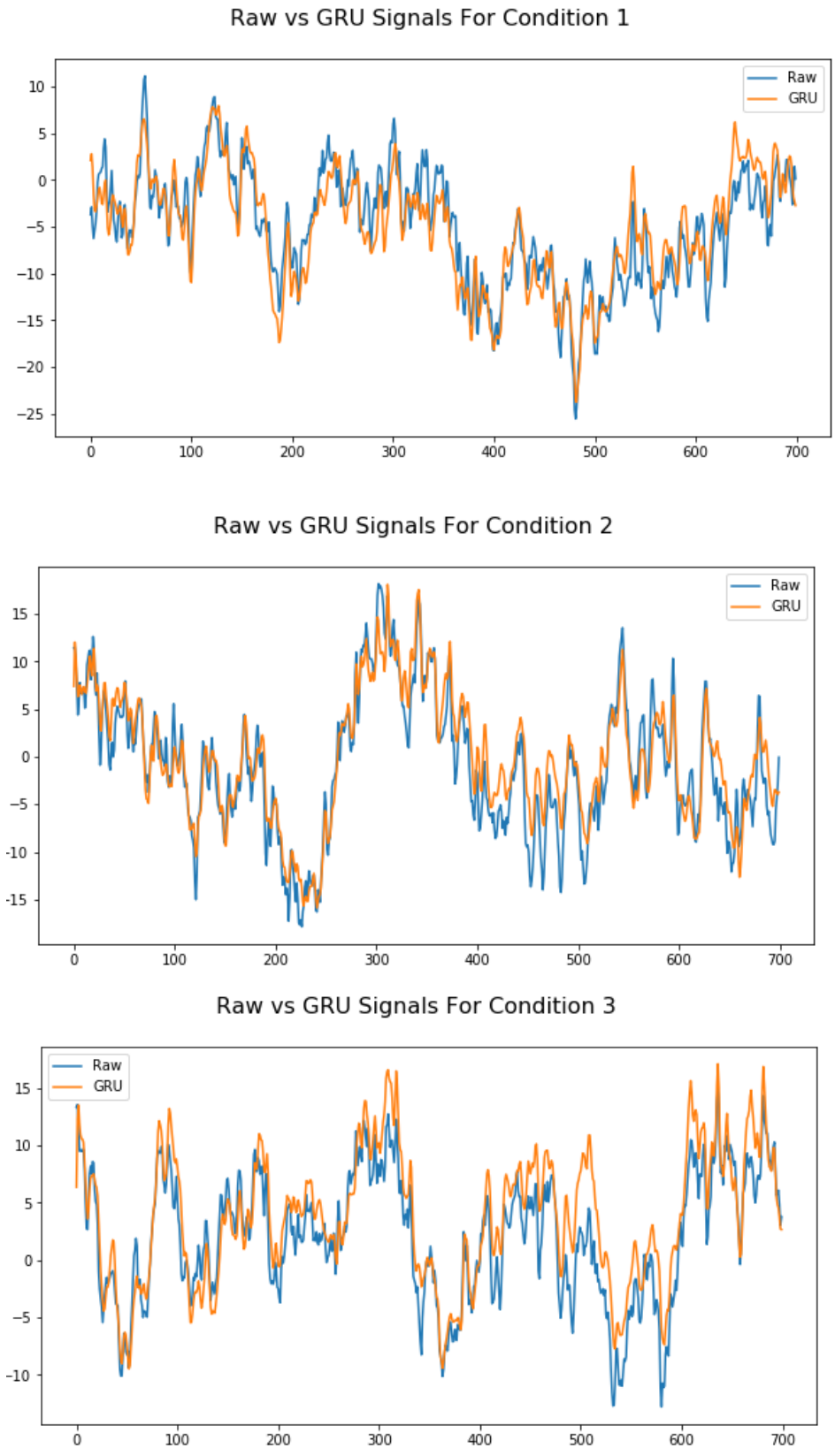

Figure 4.1.2-2 Raw vs GRU-AE reconstructed signal for each condition

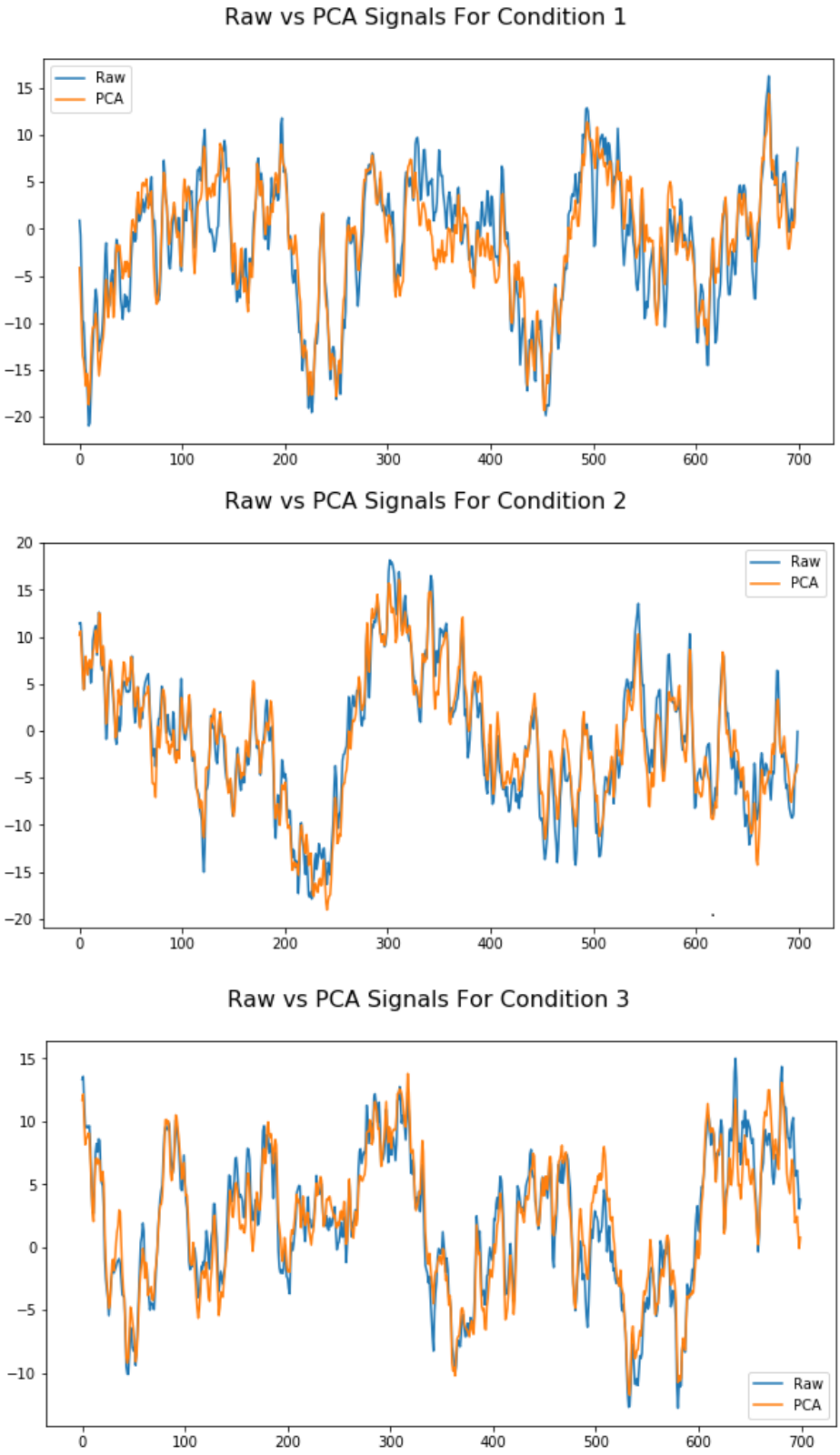

Figure 4.1.3-1 Raw vs PCA reconstructed signal for each condition

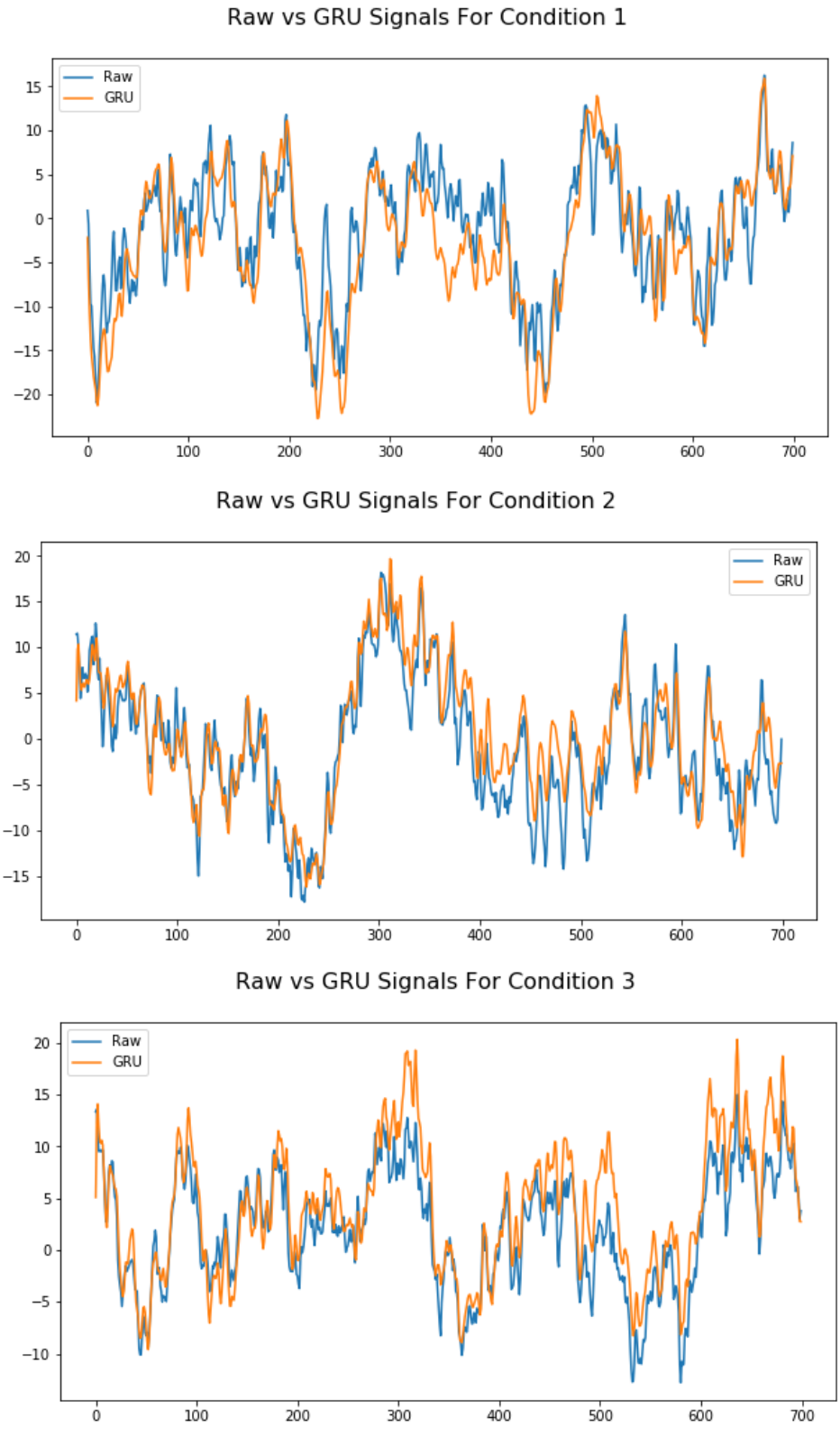

Figure 4.1.3-2 Raw vs GRU-AE reconstructed signal for each condition

4.2 Evaluation

In order to evaluate the proposed model, after the SNRs were calculated for raw signals, all reconstructed signals from 9 GRU-AE models and PCA, for each condition, Harrell-Davis decile values for the SNR distributions were calculated for 9 deciles, then the Harrell-Davis decile differences between raw signals and PCA reconstructed signals (PCA_SNRs), and Harrell-Davis decile differences between raw signals and GRU-AE reconstructed signals (GRU_SNRs) were calculated. From 9 models, the model with the highest mean difference was selected as the best model and the model with the lowest mean difference was selected as the worst performed model. Summary of the results of the Harrell-Davis decile calculations can be seen in Table 4.2-1.

Architecture	# of Neurons	Condition 1		Condition 2		Condition 3	
		# Positive differences	Mean Difference	# of Positive HD difference	Mean Difference	# of Positive HD difference	Mean Difference
Architecture 1	(64,45,64)	5	1.202	4	0.236	4	0.204
Architecture 1	(64,35,64)	6	1.476	5	0.302	4	0.354
Architecture 1	(64,25,64)	6	1.670	6	0.821	5	0.584
Architecture 2	(64,45,19,45,64)	6	2.325	5	0.830	4	0.786
Architecture 2	(64,35,29,35,64)	6	2.906	5	0.976	5	0.800
Architecture 2	(64,39,25,39,64)	6	2.557	6	0.837	4	0.428
Architecture 3	(64,58,50,45,50,58,64)	6	2.444	4	0.579	4	0.096
Architecture 3	(64,55,45,35,45,55,64)	6	2.420	4	0.626	4	0.574
Architecture 3	(64,51,38,25,38,51,64)	6	2.332	5	0.676	4	0.783

Table 4.2-1 Harrell Davis Decile Calculation Summary

Positive mean Harrell Davis decile value difference indicates that all GRU-AE models outperformed the PCA for noise reduction in all conditions which also means GRU-AE reconstructed signals have higher SNRs than the PCA reconstructed one.

For all models, it can be said that the highest mean Harrell-Davis decile differences are highest for Condition 1 and lowest for Condition 3 which means the models performed better on the Condition 1 data.

Architecture 1 with 45 neurons (64,**45**,64) was selected as the worst performed model when compared to other architectures since the mean Harrell-Davis decile difference is the lowest. Although the Architecture 1 with 45 neurons was selected as the worst performed model, as it mentioned before, it outperforms PCA. Best model was selected from Architecture 2 with (64,**35**,**29**,**35**,64) since it has the highest mean Harrell-Davis

decile difference. Summary of the structure of the best model can be found in Appendix E.

4.2.1 Condition 1

In Table 4.2-2, for Condition 1, it is shown that the mean Harrell-Davis decile difference between PCA reconstructed signals' and raw signals' SNR distribution (PCA_SNRs) is 0.175, and the mean Harrell-Davis decile difference between GRU-AE reconstructed signals' and raw signals' SNR distribution (GRU_SNRs) is 0.321. To see if the GRU-AE outperformed the PCA for noise reduction, Harrell-Davis decile differences (GRU-PCA) were divided by the related decile's PCA_SNRs. 6 deciles out of 9 have positive Harrell-Davis decile difference value, that means for that negative 3 deciles (Decile 2,3,4), PCA outperformed GRU-AE and have a higher SNR. In overall, it can be concluded that GRU-AE performed better since most of the deciles (≥ 5) have positive Harrell-Davis decile difference and the mean Harrell-Davis decile difference is positive (2.906).

It can be said that there is an evidence to support rejecting the null hypothesis.

Decile	PCA_SNRs	GRU_SNRs	GRU- PCA	(GRU-PCA)/ PCA_SNRs
1	-0.020	-0.692	-0.671	32.890
2	0.030	-0.347	-0.378	-12.511
3	0.081	-0.179	-0.261	-3.208
4	0.135	0.090	-0.045	-0.334
5	0.152	0.321	0.169	1.109
6	0.187	0.537	0.349	1.865
7	0.270	0.796	0.526	1.947
8	0.320	1.071	0.752	2.351
9	0.424	1.289	0.865	2.043
Mean	0.175	0.321	0.145	2.906

Table 4.2-2 Harrell Davis decile differences for Condition 1 (Best model)

4.2.2 Condition 2

In Table 4.2-3, for Condition 2, it is shown that the mean Harrell-Davis decile difference between PCA reconstructed signals' and raw signals' SNR distribution (PCA_SNRs) is 0.165, and the mean Harrell-Davis decile difference between GRU-AE reconstructed signals' and raw signals' SNR distribution (GRU_SNRs) is 0.172. 5 deciles out of 9 have positive Harrell-Davis decile difference value. It can be concluded that GRU-AE performed better since most of the deciles (≥ 5) have positive Harrell-Davis decile difference and the mean Harrell-Davis decile difference is positive (0.976).

It can be said that there is an evidence to support rejecting the null hypothesis.

Decile	PCA_SNRs	GRU_SNRs	GRU- PCA	(GRU-PCA)/ PCA_SNRs
1	-0.026	-0.560	-0.534	20.151
2	0.036	-0.322	-0.358	-9.817
3	0.064	-0.236	-0.300	-4.708
4	0.120	-0.019	-0.139	-1.158
5	0.125	0.121	-0.004	-0.033
6	0.199	0.275	0.076	0.383
7	0.239	0.503	0.264	1.104
8	0.304	0.712	0.408	1.345
9	0.428	1.076	0.648	1.513
Mean	0.165	0.172	0.007	0.976

Table 4.2-3 Harrell Davis decile differences for Condition 2 (Best model)

4.2.3 Condition 3

In Table 4.2-4, for Condition 3, it is shown that the mean Harrell-Davis decile difference between PCA reconstructed signals' and raw signals' SNR distribution (PCA_SNRs) is 0.163, and the mean Harrell-Davis decile difference between GRU-AE reconstructed signals' and raw signals' SNR distribution (GRU_SNRs) is 0.060. 5 deciles out of 9 have positive Harrell-Davis decile difference value. It can be concluded that GRU-AE

performed better since most of the deciles (≥ 5) have positive Harrell-Davis decile difference and the mean Harrell-Davis decile difference is positive (0.800).

It can be said that there is an evidence to support rejecting the null hypothesis.

Decile	PCA_SNRs	GRU_SNRs	GRU- PCA	(GRU-PCA)/ PCA_SNRs
1	-0.017	-0.646	-0.629	36.945
2	0.020	-0.444	-0.464	-23.118
3	0.057	-0.272	-0.329	-5.804
4	0.095	-0.138	-0.233	-2.454
5	0.171	-0.012	-0.183	-1.068
6	0.190	0.201	0.011	0.060
7	0.238	0.349	0.111	0.466
8	0.307	0.630	0.323	1.055
9	0.411	0.871	0.460	1.121
Mean	0.163	0.060	-0.104	0.800

Table 4.2-4 Harrell Davis decile differences for Condition 3 (Best model)

4.3 Discussion

In this section, strengths and the limitations of the selected model are discussed.

4.3.1 Strengths

- **Higher SNRs:** GRU-AEs performed better than the PCA. All the 9 models resulted with the positive mean Harrell-Davis decile differences.
- **Training time :** Architecture 2 required less time than Architecture 3.

4.3.2 Limitations

• **Training time**: GRU-AEs required more training time than other techniques such as PCAs, CNNs.

• **Trial-wise**: Channel-wise SNR differences cannot be visualised.

5. CONCLUSION

5.1 Research Overview

Brain is the most important organ that controls the entire body. Understanding its cognitive and functional behaviour by its electrical activity is an interesting area. Electrical activities can be measured with EEG. EEG signals are used for various tasks such as emotion recognition, seizure detection and other clinical or cognitive research. It is advantageous since it has lower costs, safe, and captures the activities in real-time. In this research EEG signal analysis is explored.

5.2 Problem Definition

Besides all the advantages, EEG signals are sensitive, they can be easily affected by the artefacts (noise) such as eye blinking, eye movement and head movement and it is nearly impossible to record clean EEG signals. Power of the noise in the signals can be measured with SNR. Increase in the SNR indicates that the noise in the signal has reduced. In EEG signal analysis, to get accurate results, it is extremely important to reduce the noise while protecting the information in the signal. Noise reduction can be done with numerous techniques from traditional such as PCA, ICA to deep learning techniques such as CNNs, RNNs and autoencoders and it is shown that they outperformed traditional techniques. Hence EEG signals are sequences, they can be treated as timeseries, LSTM based RNN and GRU based RNN, which aim to solve vanishing gradient problem caused by vanilla RNNs, proved their success on sequential data, and autoencoder with deep neural network layers showed success for noise reduction, in this research autoencoders built upon GRU based RNN layers were investigated to see if they are successful as PCA, which is used as a baseline in this research for noise reduction to increase the SNR.

5.3 Design/Experimentation, Evaluation & Results

To answer the research question "*Can a stacked autoencoder built upon Gated Recurrent Unit based Recurrent Neural Network layers (GRU-AE) perform better and have a higher signal-to- noise ratio when compared to Principal Component Analysis*

for noise reduction of electroencephalography signals?", three main architectures were designed with different number of layers, and they were manipulated by different number of neurons. As a result, totally 9 models were designed. For each condition, models were trained separately. Test sets for each condition were fed into 9 GRU-AE models and PCA. To see whether a GRU-AE increases the SNR when compared to PCA for noise reduction of EEG signals for each condition SNRs of the raw test signals and reconstructed signals were calculated. Then Harrell-Davis decile values were calculated for those SNR distributions and difference between raw test signals and reconstructed signals' SNR distributions were calculated and examined. Positive mean difference decile values indicated that GRU-AEs perform better than PCA. In overall, all GRU-AE models resulted with higher mean Harrell-Davis decile difference for SNR distributions and concluded that GRU-AE outperformed PCA. From 9 GRU-AE models, Architecture 1 with 45 neurons (64,**45**,64) was selected as the worst performed model when compared to other architectures since the mean Harrell-Davis decile difference is the lowest and Architecture 2 with (64,**35,29**,**35**,64) was selected as the best model since it has the highest mean Harrell-Davis decile difference. For the best model, for each condition, most of the deciles' mean Harrell-Davis decile difference resulted positive and compared to the PCA, it increased the SNR which are the evidences to support rejecting the null hypothesis.

5.4 Contributions and impact

From the evaluation, it can be concluded that stacked autoencoders built upon GRU based RNN layers can be used for noise reduction of EEG signals and they can increase the SNRs when compared to traditional noise reduction technique PCA. For the architecture, it can be said that making the architecture of GRU-AE deep (from Architecture 1 to Architecture 2) helps to improve the performance but it has also shown that making the architecture deeper (Architecture 2 to Architecture 3) did not improve the performance of the autoencoders.

5.5 Future Work & recommendations

In this research, SNRs were calculated by trial, channel SNRs were averaged for each trial. For future work, SNRs can be calculated by channel-wise to see the impact of the

GRU-AEs for each channel's SNR. Since the evaluation done for each condition separately, training sets were divided into three different sets for each condition which resulted with lower sample size for the training. GRU-AEs performance against PCA for noise reduction on EEG can be investigated with more than one dataset in the future.

Another interesting and challenging area of development is the application of autoencoders to remove noise from continuous EEG signals gathered in ecological settings and not constrained to stimuli. Example of ecological settings include the execution of daily tasks by participants, like searching for information on the web (Longo, Dondio & Barrett, 2010; Longo, Barrett & Dondio, 2009a; Dondio & Longo, 2011; Longo, Barrett & Dondio, 2009b) or interacting with web-sites for the sake of usability inspection (Longo, 2017; Longo, 2018a; Longo & Dondio, 2015) or even more complex mental activities performed by train drivers (Balfe, Crowley, Smith & Longo, 2017), human reasoners (Crotti, Debruyne, Longo & O'Sullivan, 2019; Dondio & Longo, 2014), teachers and learners (Longo, 2018b; Orru, Gobbo, O'Sullivan & Longo, 2018) exposed to continuous exertion of effort (Longo & Barrett, 2010) and mental workload (Longo, 2015; Rizzo & Longo, 2017; Rizzo & Longo, 2018; Orru & Longo, 2019).

Also, the use of transformer based variational autoencoders, which are the state-of-art for some Natural Language Processing tasks (Liu & Liu, 2019), can be investigated for noise reduction of EEG signals to see whether they can increase the SNRs when compared to GRU-AEs.

Lastly, for the supervised deep learning tasks, such as emotion recognition from EEG signals (Soleymani et al., 2014; Alhagry et al., 2017), GRU-AE (Cowton, Kyriazakis, Plötz & Bacardit, 2018), traditional or other deep learning techniques for noise reduction can be used for reconstruction then they can be fed into classifiers to compare the classification results.

BIBLIOGRAPHY

Abbas, W. & Khan, N.A. (2018). DeepMI: deep learning for multiclass motor imagery classification. *2018 40th Annual International Conference of the IEEE Engineering in Medicine and Biology Society (EMBC),* 219-222. doi:10.1109/EMBC.2018.8512271

Acharya, U.R., Oh, S.L., Hagiwara, Y., Tan, J.H. & Adeli, H. (2018). Deep convolutional neural network for the automated detection and diagnosis of seizure using EEG signals. *Computers in Biology and Medicine, 100*(1), 270-278. doi:10.1016/j.compbiomed.2017.09.017

Adeli, H., Zhou, Z., & Dadmehr, N. (2003). Analysis of EEG records in an epileptic patient using wavelet transform. *Journal of Neuroscience Methods, 123*(1), 69–87. doi:10.1016/S0165-0270(02)00340-0

Affes, A., Mdhaffar, A., Triki, C., Jmaiel, M. & Freisleben, B. (2019). A convolutional gated recurrent neural network for epileptic seizure prediction. In: Pagán J., Mokhtari M., Aloulou H., Abdulrazak B., Cabrera M. (eds), *Lecture Notes in Computer Science: Vol. 11862, How AI Impacts Urban Living and Public Health. ICOST 2019* (85-96). Cham: Springer. doi:10.1007/978-3-030-32785-9_8

Ahmad, T., Fairuz, R.A., Zakaria, F. & Isa, H. (2008). Selection of a subset of EEG channels of epileptic patient during seizure using PCA. *Proceedings of the 7th WSEAS International Conference on Signal Processing, Robotics and Automation (ISPRA '08),* 270-273. Retrieved from https://pdfs.semanticscholar.org/2b14/685ebcb545ddb4235031e467df45b10b324e.pdf

Ahmedt-Aristizabal, D., Fookes, C., Nguyen, K. & Sridharan, S. (2018). Deep classification of epileptic signals. *2018 40th Annu. Int. Conf. IEEE Eng. Med. Biol. Soc. (EMBC),* 332–335. doi:10.1109/EMBC.2018.8512249

Akhtar M.T., Mitsuhashi, W. & James, C.J. (2012). Employing spatially constrained ICA and wavelet denoising, for automatic removal of artifacts from multichannel EEG data. *Signal Processing, 92*(1), 401-416. doi:10.1016/j.sigpro.2011.08.005

Alegre, M., Labarga, A., Gurtubay, I., Iriarte, J., Malanda, A. & Artieda, J. (2003). Movement-related changes in cortical oscillatory activity in ballistic, sustained and negative movements. *Experimental Brain Research, 148*(1), 17–25. doi:10.1007/s00221-002-1255-x

Alhagry, S., Fahmy, A.A. & El-Khoribi, R. (2017). Emotion recognition based on EEG using LSTM recurrent neural network, *International Journal of Advanced Computer Science and Applications, 8*(10), 355-358. doi:10.14569/IJACSA.2017.081046

Aminghafari, M., Cheze, N. & Poggi, J-M., Multivariate denoising using wavelets and principal component analysis. *Computational Statistics & Data Analysis, 50*(9), 2381–2398. doi:10.1016/j.csda.2004.12.010

Antoniades, A., Spyrou, L., Took. C.C. & Sanei, S. (2016). Deep learning for epileptic intracranial EEG data. *2016 IEEE 26th International Workshop on Machine Learning for Signal Processing (MLSP)*, 1-6, doi:10.1109/MLSP.2016.7738824

Artoni, F., Delorme, A. & Makeig, S. (2018). Applying dimension reduction to EEG data by principal component analysis reduces the quality of its subsequent Independent Component decomposition. *Neuroimage, 175*(1), 176-187. doi:10.1016/j.neuroimage.2018.03.016

Aznan, N.K.N., Atapour-Abarghouei, A., Bonner, S., Connolly, J.D., Al Moubayed, N. & Breckon, T.P. (2019). Simulating brain signals: creating synthetic EEG data via neural-based generative models for improved SSVEP classification. *2019 International Joint Conference on Neural Networks (IJCNN)*, 1-8. doi:10.1109/IJCNN.2019.8852227

Balfe, N., Crowley, K., Smith, B. & Longo, L. (2017). Estimation of train driver workload: extracting taskload measures from on-train-data-recorders. *International Symposium on Human Mental Workload: Models and Applications*, *726*(1), 106-119. doi:10.1007/978-3-319-61061-0_7

Bi, L., Zhang, J. & Lian, J. (2019). EEG-based adaptive driver-vehicle interface using variational autoencoder and PI-TSVM. *IEEE Transactions on Neural Systems and Rehabilitation Engineering*, *27*(10), 2025-2033. doi:10.1109/TNSRE.2019.2940046

Bresch, E., Großekathöfer, U. & Garcia-Molina, G. (2018). Recurrent deep neural networks for real-time sleep stage classification from single channel EEG *Frontiers in Computational Neuroscience, 12*;85, 1-12. doi:10.3389/fncom.2018.00085

Bromm, B. & Scharein, E. (1982). Principal component analysis of pain-related cerebral potentials to mechanical and electrical stimulation in man. *Electroencephalography and Clinical Neurophysiology, 53*(1). 94–103. doi:10.1016/0013-4694(82)90109-2

Cao, L.J., Chua, K.S., Chong, W.K., Lee, H.P. & Gu, Q.M. (2003). A comparison of PCA, KPCA and ICA for dimensionality reduction in support vector machine. *Neurocomputing 55*(1-2), 321-336. doi:10.1016/S0925-2312(03)00433-8

Casarotto, S., Bianchi, A.M., Cerutti, S. & Chiarenza, G.A. (2004). Principal component analysis for reduction of ocular artefacts in event-related potentials of normal and dyslexic children. *Clinical Neurophysiology, 115*(1). 609-619. doi:10.1016/j.clinph.2003.10.018

Cho, K., van Merriënboer, B., Gulcehre, C., Bougares, F., Schwenk, H., & Bengio, Y. (2014). Learning phrase representations using RNN encoder-decoder for statistical machine translation. In *Proceedings of the Empirical Methods in Natural Language Processing (EMNLP 2014)*. 1724 – 1734. Retrieved from https://www.aclweb.org/anthology/D14-1179.pdf

Choi, G., Park, C., Kim, J., Cho, K. & Kim, T-J. (2019). A novel multi-scale 3D CNN with deep neural network for epileptic seizure detection. *2019 IEEE International Conference on Consumer Electronics (ICCE),* 1-2. doi:10.1109/ICCE.2019.8661969

Comon, P. (1994). Independent component analysis: a new concept? *Signal Process, 36*(1), 287–314. doi:10.1016/0165-1684(94)90029-9

Cowton, J., Kyriazakis, I., Plötz, T. & Bacardit, J. (2018). A combined deep learning GRU-autoencoder for the early detection of respiratory disease in pigs using multiple environmental sensors. *Sensors*, *18,* 2521. 1-20. doi: 10.3390/s18082521

Craik, A., He, Y. & Contreras-Vidal, J.L. (2019). Deep learning for electroencephalogram (EEG) classification tasks: a review. *Journal of Neural Engineering, 16*(3), 1-28. doi:10.1088/1741-2552/ab0ab5

Crespo-Garcia, M., Atienza, M. & Cantero, J.L. (2008). Muscle artifact removal from human sleep EEG by using independent component analysis. *Annals of Biomedical Engineering, 36*(3), 467-475. doi:10.1007/s10439-008-9442-y

Crotti, A., Jr., Debruyne, C., Longo, L. & O'Sullivan, D. (2019). On the mental workload assessment of uplift mapping representations in linked data. In Longo L., Leva M. (eds), *Human Mental Workload: Models and Applications.* (pp.160-179). Cham: Springer International Publishing. doi:10.1007/978-3-030-14273-5_10

Dai, M., Zheng, D., Na, R., Wang, S. & Zhang, S. (2019). EEG classification of motor imagery using a novel deep learning framework. *Sensors, 19*(3); 551, 1-16. doi:10.3390/s19030551

Davidson, P.R., Jones, R.D., & Peiris M.T.R. (2007). EEG-based lapse detection with high temporal resolution. *IEEE Transactions on Biomedical Engineering, 54*(5), 832-839. doi:10.1109/TBME.2007.893452

Delorme, A. & Makeig, S. (2004) EEGLAB: an open source toolbox for analysis of single-trial EEG dynamics including independent component analysis. *Journal of neuroscience methods, 134*(1), 9–21.doi:10.1016/j.jneumeth.2003.10.009

Dondio, P. & Longo, L. (2011). Trust-based techniques for collective intelligence in social search systems. In *Next Generation Data Technologies for Collective Computational Intelligence, Vol. 352* (pp. 113-135). doi:10.1007/978-3-642-20344-2_5

Dondio, P. & Longo, L. (2014). Computing trust as a form of presumptive reasoning. In *2014 IEEE/WIC/ACM International Joint Conferences on Web Intelligence (WI) and Intelligent Agent Technologies (IAT), 2*(1), 274-281. doi:10.1109/WI-IAT.2014.108

Dong, G., Liao, G., Liu, H. & Kuang, G. (2018). A review of the autoencoder and its variants: a comparative perspective from target recognition in synthetic-aperture radar images. *IEEE Geoscience and Remote Sensing Magazine*, *6*(3), 44-68. doi:10.1109/MGRS.2018.2853555

Emami, A., Kunii, N., Matsuo, T., Shinozaki, T., Kawai, K. & Takahashi, H. (2019). Seizure detection by convolutional neural network-based analysis of scalp electroencephalography plot images. *NeuroImage: Clinical, 22*(1); 1016843, 1-10. doi:10.1016/j.nicl.2019.101684

Flexer, A., Bauer, H., Pripfl, J. & Dorffner, G. (2005). Using ICA for removal of ocular artifacts in EEG recorded from blind subjects. *Neural Networks, 18*(7), 998-1005. doi:10.1016/j.neunet.2005.03.012

Foresta, F.L., Morabito, F.C., Marino, S. & Dattola, S. (2019). High-density EEG signal processing based on active-source reconstruction for brain network analysis in alzheimer's disease. *Electronics, 8*(9), 1031-1045. doi:10.3390/electronics8091031

Ford, J. M., Palzes, V. A., Roach, B. J., & Mathalon, D. H. (2013). Did I do that? abnormal predictive processes in schizophrenia when button pressing to deliver a tone. *Schizophrenia Bulletin, 40*(4), 804–812. doi:10.1093/schbul/sbt072

Friedman, D., & Johnson, R. (2000). Event-related potential (ERP) studies of memory encoding and retrieval: A selective review. *Microscopy Research and Technique*, *51*(1), 6-28. doi:10.1002/1097-0029(20001001)51:1<6::AID-JEMT2>3.0.CO;2-R

Frølich, L. & Dowding, I. (2018). Removal of muscular artifacts in EEG signals: a comparison of linear decomposition methods. *Brain Informatics, 5*(1), 13-22. doi:10.1007/s40708-017-0074-6

Fukushima, K. (1980). Neocognitron: a self-organizing neural network model for a mechanism of pattern recognition unaffected by shift in position. *Biological Cybernetics, 36*(1) , 193-202. doi:10.1007/BF00344251

Ghandeharion, H. & Erfanian, A. (2010). A fully automatic ocular artifact suppression from EEG data using higher order statistics: improved performance by wavelet analysis. *Medical Engineering & Physics, 32*(7), 720–729. doi:10.1016/j.medengphy.2010.04.010

Goelz, H., Jones, R. & Bones, P. (2000). Wavelet analysis of transient biomedical signals and its application to detection of epileptiform activity in the EEG. *Clinical Electroencephalography, 31*(4), 181–191. doi:10.1177/155005940003100406

Golmohammadi, M., Ziyabari, S., Shah, V., Weltin, E.V., Campbell, C., Obeid, I. & Picone, J. (2017). Gated recurrent networks for seizure detection. *2017 IEEE Signal Processing in Medicine and Biology Symposium (SPMB),* 1-5. doi:10.1109/SPMB.2017.8257020

Goodfellow, I., Bengio, Y. & Courville, A. (2016). *Deep Learning.* MIT Press.

Graves, A. (2012). *Supervised Sequence Labelling with Recurrent Neural Networks.* Berlin: Springer.

Grossman, A., & Morlet, J. (1985). Decompositions of functions into wavelets of constant shape and related transforms. In L. Streit (Ed.), *Mathematics + Physics,* 135-165. Singapore: World Scientific.

Haas, L F. (2003). "Hans Berger (1873-1941), Richard Caton (1842-1926), and electroencephalography". *Journal of Neurology, Neurosurgery & Psychiatry. 74*(1)*,* 7-9. doi:10.1136/jnnp.74.1.9

Hair, J., Anderson, R., Tatham, R., & Black, W. (1995). *Multivariate data analysis (4th ed.).* New Jersey: Prentice-Hall.

Hajinoroozi, M., Mao, Z., Jung, T-P., Lin, C-T. & Huang, Y. (2016). EEG-based prediction of driver's cognitive performance by deep convolutional neural network. *Signal Processing: Image Communication 47*(1), 549–555. doi:10.1016/j.image.2016.05.018

Harrell, F.E. & Davis, C.E. (1982). A new distribution-free quantile estimator. *Biometrika,69*(3)*,* 635-640. doi:10.1093/biomet/69.3.635.

Haufe, S., Dahne, S. & Nikulin, V. (2014). Dimensionality reduction for the analysis of brain oscillations. *NeuroImage, 101*(1), 583-597. doi:10.1016/j.neuroimage.2014.06.073

Hefron, R., Borghetti, B., Kabban, C.S., Christensen, J. & Estepp, J. (2018). Cross-participant EEG-based assessment of cognitive workload using multi-path convolutional recurrent neural networks. *Sensors, 18*(5);1339, 1-27. doi:10.3390/s18051339

Helal, M.A., Eldawlatly, S. & Taher, M. (2017). Using autoencoders for feature enhancement in motor imagery brain-computer interfaces. *Proceedings of the IASTED International Conference Biomedical Engineering (BioMed 2017),* 89-93. doi: 10.2316/P.2017.852-052

Herault, J., Jutten, C. (1986). Space or time adaptative signal processing by neural networks models. *Proceedings of the International Conference, 151*(1), 206–211. doi:10.1063/1.36258

Heydari, E. & Shahbakhti, M. (2015). Adaptive wavelet technique for EEG de-noising. *8th Biomedical Engineering International Conference (BMEiCON-2015),* 1-4. doi:10.1109/BMEiCON.2015.7399503

Hochreiter, S. & Schmidhuber, J. (1997). Long short-term memory. *Neural Computation*, *9*(8), 1735–1780. doi:10.1162/neco.1997.9.8.1735

Homan, R.W., Herman, J. & Purdy, P. (1987). Cerebral location of international 10-20 system electrode placement. *Electroencephalography and clinical neurophysiology*, *66*(4), 376-382. doi:10.1016/0013-4694(87)90206-9

Hosseini, M-P., Soltanian-Zadeh, H., Elisevich, K. & Pompili, D. (2017). Cloud-based deep learning of big EEG data for epileptic seizure prediction. *2016 IEEE Global Conference on Signal and Information Processing,* 1151-1155. doi:10.1109/GlobalSIP.2016.7906022

Hubel, D. H., & Wiesel, T. N. (1968). Receptive fields and functional architecture of monkey striate cortex. *The Journal of Physiology, 195*(1), 215–243. doi:10.1113/jphysiol.1968.sp008455

Hussein, R., Palangi, H., Ward. R.K. & Wang, Z.J. (2019). Optimized deep neural network architecture for robust detection of epileptic seizures using EEG signals. *Clinical Neurophysiology, 130*(1), 25-37. doi:10.1016/j.clinph.2018.10.010

Indiradevi, K.P., Elias, E., Sathidevi, P.S., Dinesh Nayak, S. & Radhakrishnan, K.A. (2008). A multi-level wavelet approach for automatic detection of epileptic spikes in the electroencephalogram. *Computers in Biology and Medicine, 38*(7), 805–816. doi:10.1016/j.compbiomed.2008.04.010

Iriarte, J., Urrestarazu, J., Valencia, M., Alegre, M., Malanda, A., Viteri, C. & Artieda, J. (2003). Independent component analysis as a tool to eliminate artifacts in EEG: a quantitative study. *Journal of Clinical Neurophysiology. 20*(4), 249–257. doi:10.1097/00004691-200307000-00004

Iyer, D. & Zouridakis, G. (2007). Single-trial evoked potential estimation: comparison between independent component analysis and wavelet denoising. *Clinical Neurophysiology, 118*(3), 495–504. doi:10.1016/j.clinph.2006.10.024

Jafarifarmand, A. & Badamchizadeh, M. A. (2013). Artifacts removal in EEG signal using a new neural network enhanced adaptive filter. *Neurocomputing*, *103*(1), 222-231. doi:10.1016/j.neucom.2012.09.024

James, C.J., Kobayashi, K. & Lowe, D. (1999) Isolating epileptiform discharges in the unaveraged EEG using independent component analysis. *IEE Colloquium on Medical Applications of Signal Processing (Ref. No. 1999/107)*, 2/1-2/6. Retrieved from http://ieeexplore.ieee.org/stamp/stamp.jsp?tp=&arnumber=828600&isnumber=17994

James, C.J. & Gibson, O.J. (2003). Temporally constrained ICA: an application to artifact rejection in electromagnetic brain signal analysis. *IEEE Transactions on Biomedical Engineering, 50*(9), 1108-1116. doi:10.1109/TBME.2003.816076

Jasper, H.H. (1958). Report of the committee on methods of clinical examination in electroencephalography. *Electroencephalography and Clinical Neurophysiology*, *10*(2), 370–375. doi:10.1016/0013-4694(58)90053-1

Jiao, Z., Gao, X., Wang, Y., Li, J. & Xu, H. (2018). Deep convolutional neural networks for mental load classification based on EEG data. *Pattern Recognition*, *76*(1), 582-595. doi:10.1016/j.patcog.2017.12.002

Jirayucharoensak, S., Pan-Ngum, S. & Israsena, P. (2014). EEG-based emotion recognition using deep learning network with principal component based covariate shift adaptation, *Scientific World Journal,* 627892, 1-10. doi:10.1155/2014/627892

Johnson, Jr.R. (1992). Event-related brain potentials. *Progressive supranuclear palsy: Clinical and research approaches*, *6*(2), 122-154.

Joyce, C.A., Gorodnitsky, I.F. & Kutas, M. (2004). Automatic removal of eye movement and blink artifacts from EEG data using blind component separation. *Psychophysiology, 41*(1), 313–325. doi:10.1046/j.1469-8986.2003.00141.x

Jung, T-P., Humphries, C., Lee, T.-W., Makeig, S., McKeown, M. J., Iragui, V., & Sejnowski, T.J. (1997). Extended lCA removes artifacts from electroencephalographic recordings. *NIPS'97 Proceedings of the 10th International Conference on Neural Information Processing Systems,* 894-900. Denver: MIT Press.

Jung, T-P., Makeig, S., Humphries, C., Lee, T-W., McKeown, M.J., Iragui, V. & Sejnowski, T.J. (2000). Removing electroencephalographic artifacts by blind source separation. *Psychophysiology, 37*(2), 163–178. doi:10.1111/1469-8986.3720163

Kan, D.P., & Lee, P.F. (2015). Decrease alpha waves in depression: an electroencephalogram (EEG) study. *2015 International Conference on BioSignal Analysis, Processing and Systems*, 156-161. doi:10.1109/ICBAPS.2015.7292237

Kaushal, G., Singh, A. & Jain, V. (2016). Better approach for denoising EEG signals. *2016 5th International Conference on Wireless Networks and Embedded Systems (WECON),*1-3. doi:10.1109/WECON.2016.7993455

Kevric, J. & Subasi, A. (2014). The effect of multiscale PCA de-noising in epileptic seizure detection*, Journal of Medical Systems, 38*(10), 131 - 144. doi:10.1007/s10916-014-0131-0

Khatwani, P. & Tiwari, A. (2013). A survey on different noise removal techniques of EEG signals. *International Journal of Advanced Research in Computer and Communication Engineering, 2*(2), 1091-1095. doi:10.17148/IJARCCE

Kobayashi, T., Kuriki, S. (1999). Principal component elimination method for the improvement of S/N in evoked neuromagnetic field measurements. *IEEE Transactions on Biomedical Engineering, 46*(8), 951–958. doi:10.1109/10.775405

Krishnaveni, V., Jayaraman, S., Anitha, L., Ramadoss, K. (2006). Removal of ocular artifacts from EEG using adaptive thresholding of wavelet coefficients. *Journal of Neural Engineering, 3*(4), 338–346. doi:10.1088/1741-2560/3/4/011

Kuanar, S., Athitsos, V., Pradhan, N., Mishra, A. & Rao, K.R. (2018). Cognitive analysis of working memory load from EEG, by a deep recurrent neural network. *2018 IEEE Int. Conf. on Acoustics, Speech and Signal Processing (ICASSP),* 2576–2580. doi:10.1109/ICASSP.2018.8462243

Kumar, J.S. & Bhuvaneswari, P. (2012). Analysis of electroencephalography (EEG) signals and its categorization - a study. *Procedia Engineering, 38*(1), 2525-2536. doi:10.1016/j.proeng.2012.06.298

Kumar, P.S., Arumuganathan, R., Sivakumar, K. &Vimal, C. (2008). Removal of artifacts from EEG signals using adaptive filter through wavelet transform*, 2008 9th International Conference on Signal Processing,* 2138-2141. doi:10.1109/ICOSP.2008.4697569

Lagerlund, T.D., Sharbrough, F.W. & Busacker, N.E. (1997). Spatial filtering of multichannel electroencephalographic recordings through principal component analysis by singular value decomposition. *Journal of Clinical Neurophysiology, 14*(1), 73–82. doi:10.1097/00004691-199701000-00007

Lau, T.M., Gwin, J.T. & Ferris, D.P. (2012). How many electrodes are really needed for EEG-based mobile brain imaging? *Journal of Behavioral and Brain Science, 2*(3), 387-393. doi:10.4236/jbbs.2012.23044

Lauzon, F.Q. (2012). An introduction to deep learning. *International Conference on Information Science, Signal Processing and their Applications (ISSPA)*, 1438-1439. doi:10.1109/ISSPA.2012.6310529

LeCun, Y. (1989). Generalization and network design strategies. Technical Report CRG-TR-89-4, University of Toronto.

LeCun, Y., Kavukcuoglu, K. & Farabet, C. (2010). Convolutional networks and applications in vision. *Proceedings of 2010 IEEE International Symposium on Circuits and Systems*, 253-256. doi:10.1109/ISCAS.2010.5537907

Leeuwen, K.G., Sun, H., Tabaeizadeh, M., Struck, A.F., & Westover, M.B. (2019). Detecting abnormal electroencephalograms using deep convolutional networks. *Clinical Neurophysiology, 130*(1), 77-84. doi:10.1016/j.clinph.2018.10.012

Leite, N.M.N., Pereira, E.T., Gurjao, E.C., & Veloso, L.R. (2018). Deep convolutional autoencoder for EEG noise filtering. 2018 *IEEE International Conference on Bioinformatics and Biomedicine (BIBM)*, 2605-2612. doi:10.1109/BIBM.2018.8621080

Li, G., Lee, C.H., Jung, J.J., Youn, Y.C. & Camacho, D. (2019). Deep learning for EEG data analytics: a survey. *Concurrency and Computation: Practice and Experience*, 1-13. doi:10.1002/cpe.5199

Li, X., Song, D., Zhang, P., Yu, G., Hou, Y. & Hu, B. (2016). Emotion recognition from multi-channel EEG data through convolutional recurrent neural network. *2016 IEEE Int. Conf. Bioinformatics Biomedicine,* 352–359. doi:10.1109/BIBM.2016.7822545

Li, Y., Huang, J., Zhou, H. & Zhong, N. (2017). Human emotion recognition with electroencephalographic multidimensional features by hybrid deep neural networks. *Appl. Sci. 7*(10);1060, 1-20. doi:10.3390/app7101060

Liang, J., Lu, R., Wang, F. & Zhang, C. (2016). Predicting seizures from electroencephalography recordings: a knowledge transfer strategy. *IEEE International Conference on Healthcare Informatics (ICHI),* 184-191. doi:10.1109/ICHI.2016.27

Lin, Q., Ye, S., Huang, X., Li, S., Zhang, M., Xue, Y., & Chen, W. (2016). Classification of epileptic EEG signals with stacked sparse autoencoder based on deep learning. In Huang DS., Han K., Hussain A. (eds), Lecture Notes in Computer Science: *Vol. 9773, International Conference on Intelligent Computing* (pp. 802-810). Cham: Springer. doi:10.1007/978-3-319-42297-8_74

Liu, D. & Liu, G. (2019). A transformer-based variational autoencoder for sentence generation. *2019 International Joint Conference on Neural Networks (IJCNN),*19705, 1-7. doi:10.1109/IJCNN.2019.8852155

Longo, L. (2015). Designing medical interactive systems via assessment of human mental workload. *2015 IEEE 28th International Symposium on Computer-Based Medical Systems (CBMS),* 364-365. doi:10.1109/CBMS.2015.67

Longo, L. (2017). Subjective usability, mental workload assessments and their impact on objective human performance. In Bernhaupt R., Dalvi G., Joshi A., K. Balkrishan D., O'Neill J., Winckler M. (eds) *Human-Computer Interaction - INTERACT 2017. INTERACT 2017. Lecture Notes in Computer Science, Vol. 10514* (pp. 202-223). Cham: Springer. doi:10.1007/978-3-319-67684-5_13

Longo, L. (2018a). Experienced mental workload, perception of usability, their interaction and impact on task performance. *PLoS ONE, 13*(8), 1-36. doi:10.1371/journal.pone.0199661

Longo, L. (2018b). On the reliability, validity and sensitivity of three mental workload assessment techniques for the evaluation of instructional designs: a case study in a third-level course. In *Proceedings of the 10th International Conference on Computer Supported Education, CSEDU 2018, 2*(1), 166-178. doi:10.5220/0006801801660178

Longo, L. & Barrett, S. (2010). Cognitive effort for multi-agent systems. *International Conference on Brain Informatics, 6334*(1), 55-66. doi:10.1007/978-3-642-15314-3_6

Longo, L., Barrett, S. & Dondio, P. (2009a). Information foraging theory as a form of collective intelligence for social search. In *Computational Collective Intelligence. Semantic Web, Social Networks and Multiagent Systems* (pp. 63–74). Springer. doi:10.1007/978-3-642-04441-0_5

Longo, L., Barrett, S. & Dondio, P. (2009b). Toward social search - from explicit to implicit collaboration to predict users' interests. In *Proceedings of the Fifth International Conference on Web Information Systems and Technologies (WEBIST 2009)*. 693-696. doi:10.5220/0001841406840687

Longo, L. & Dondio, P. (2015). On the relationship between perception of usability and subjective mental workload of web interfaces. In *2015 IEEE/WIC/ACM International Conference on Web Intelligence and Intelligent Agent Technology (WI-IAT).* 345-352. doi:10.1109/WI-IAT.2015.157

Longo, L., Dondio, P. & Barrett, S. (2010). Enhancing social search: a computational collective intelligence model of behavioural traits, trust and time. *Transactions on computational collective intelligence II,* 46-69. Springer. doi:10.1007/978-3-642-17155-0_3

Luck, S. J. (2005). An introduction to the event-related potential technique. MIT Press.

Luo, T.J., Zhou, C.L. & Chao, F. (2018). Exploring spatial-frequency-sequential relationships for motor imagery classification with recurrent neural network. *BMC Bioinformatics, 19*(1);344, 1-18. doi:10.1186/s12859-018-2365-1

Luo, Y. & Wan, Y. (2013). A novel efficient method for training sparse auto-encoders. *2013 6th International Congress on Image and Signal Processing (CISP)*, 1019-1023. doi:10.1109/CISP.2013.6745205

Ma, X., Qiu, S., Du, C., Xing, J. & He, H. (2018). Improving EEG-based motor imagery classification via spatial and temporal recurrent neural networks. *2018 40th Annu. Int. Conf. IEEE Eng. Med. Biol. Soc. (EMBC),* 1903–1906. doi:10.1109/EMBC.2018.8512590

Maddirala, A.K. & Shaik, T.A. (2016). Removal of EOG artifacts from single channel EEG signals using combined singular spectrum analysis and adaptive noise canceler. *IEEE SENSORS JOURNAL, 16*(23), 8279-8287.doi:10.1109/JSEN.2016.2560219

Mahajan, R., & Morshed, B. I. (2015). Unsupervised eye blink artifact denoising of EEG data with modified multiscale sample entropy, kurtosis, and wavelet-ICA. *IEEE Journal of Biomedical and Health Informatics, 19*(1), 158-165. doi:10.1109/jbhi.2014.2333010

Michielli, N., Acharya, U.R. & Molinari, F. (2019). Cascaded LSTM recurrent neural network for automated sleep stage classification using single-channel EEG signals. *Computers in Biology and Medicine, 106*(1), 71-81. doi:10.1016/j.compbiomed.2019.01.013

Minasyan, G.R., Chatten, J.B., Chatten, M.J. & Harner, R.N. (2010). Patient-specific early seizure detection from scalp EEG. *Journal of Clinical Neurophysiology, 27*(3), 163-178. doi:10.1097/WNP.0b013e3181e0a9b6

Mirowski, P., Madhavan, D., LeCun, Y. & Kuzniecky, R. (2009). Classification of patterns of EEG synchronization for seizure prediction. *Clinical Neurophysiology, 120*(11), 1927-1940. doi:10.1016/j.clinph.2009.09.002

Mitchell, T. M. (1997). *Machine Learning.* New York: McGraw-Hill.

Mormann, F., Fell, J., Axmacher, N., Weber, B., Lehnertz, K., Elger, C.E. & Fernandez, G. (2005). Phase/amplitude reset and theta-gamma interaction in the human medial temporal lobe during a continuous word recognition memory task. *Hippocampus, 15*(7), 890–900. doi:10.1002/hipo.20117

M'ng, J.C.P. & Mehralizadeh, M. (2016). Forecasting east asian indices Futures via a novel hybrid of wavelet-PCA denoising and artificial neural network models. *PLoS One, 11*(6), 1-29. doi:10.1371/journal.pone.0156338

Narejo, S., Pasero, E. & Kulsoom, F. (2016). EEG based eye state classification using deep belief network and stacked autoencoder. *International Journal of Electrical and Computer Engineering (IJECE), 6*(6), 3131-3141. doi:10.11591/ijece.v6i6.12967

Ni, Z., Yuksel, A.C., Ni, X., Mandel, M.I. & Xie, L. (2017). Confused or not confused?: disentangling brain activity from EEG data using bidirectional LSTM recurrent neural networks. *Proceedings of the 8th ACM International Conference on Bioinformatics, Computational Biology, and Health Informatics (ACM-BCB),* 241-246. doi:10.1145/3107411.3107513

Niedermeyer, E. & da Silva, F.L. (2005). *Electroencephalography: basic principles, clinical applications, and related fields.* Amsterdam: Lippincott Williams & Wilkins.

Orru, G., Gobbo, F., O'Sullivan, D. & Longo, L. (2018). An investigation of the impact of a social constructivist teaching approach, based on trigger questions, through measures of mental workload and efficiency. In *Proceedings of the 10th International Conference on Computer Supported Education (CSEDU 2018), 2*(1), 292-302. doi:10.5220/0006790702920302

Orru, G. & Longo, L. (2019). The evolution of cognitive load theory and the measurement of its intrinsic, extraneous and germane loads: a review. In Longo L., Leva M. (eds), *Human Mental Workload: Models and Applications. H-WORKLOAD 2018. Communications in Computer and Information Science*: *Vol. 1012* (pp.23-48). Cham: Springer. doi:10.1007/978-3-030-14273-5_3

Page, A., Shea, C. & Mohsenin, T. (2016). Wearable seizure detection using convolutional neural networks with transfer learning. *2016 IEEE International Symposium on Circuits and Systems (ISCAS)*, Montreal, QC, 1086-1089. doi:10.1109/ISCAS.2016.7527433

Pearson, K. (1901). On lines and planes of closest fit to systems of points in space. *Philosophical Magazine Series 6, 2*(11), 559-572. doi:10.1080/14786440109462720

Peng, H., Hu, B., Shi, Q., Ratcliffe, M., Zhao, Q., Qi, Y., & Gao, G. (2013). Removal of ocular artifacts in EEG - an improved approach combining DWT and ANC for portable applications. *IEEE Journal of Biomedical and Health Informatics, 17*(3), 600-307. doi:10.1109/JBHI.2013.2253614

Qiao, R., Qing, C., Zhang, T., Xing, X. & Xu, X. (2017). A novel deep-learning based framework for multi-subject emotion recognition. *ICCSS 2017—2017 Int. Conf. Information, Cybernetics and Computational Social Systems*, 181-185. doi:10.1109/ICCSS.2017.8091408

Qiu, Y., Zhou, Y., Yu, N & Du, P. (2018). Denoising sparse autoencoder-based ictal EEG classification. In *IEEE Transactions on Neural Systems and Rehabilitation Engineering*, *26*(9), 1717-1726. doi:10.1109/TNSRE.2018.2864306

Radüntz, T., Scouten, J., Hochmuth, O. & Meffert, B. (2017). Automated EEG artifact elimination by applying machine learning algorithms to ICA-based features. *Journal of Neural Engineering, 14*(4):*046004*, 1-8. doi:10.1088/1741-2552/aa69d1

Rizzo, L. & Longo, L. (2017). Representing and inferring mental workload via defeasible reasoning: a comparison with the NASA task load index and the workload profile. *Proceedings of the 1st Workshop on Advances In Argumentation In Artificial Intelligence,* 1-15. Retrieved from https://pdfs.semanticscholar.org/e90c/6485b309a8c338128ee155e06b40a982a218.pdf

Rizzo, L. & Longo, L. (2018). Inferential models of mental workload with defeasible argumentation and non-monotonic fuzzy reasoning: a comparative study. In *2nd Workshop on Advances In Argumentation In Artificial Intelligence*, 11-26. Retrieved from https://arrow.tudublin.ie/cgi/viewcontent.cgi?article=1262&context=scschcomcon

Romero, S., Mananas, M.A., Clos, S., Gimenez, S. & Barbanoj, M.J. (2003). Reduction of EEG artifacts by ICA in different sleep stages. *Proceedings of the 25th Annual International Conference of the IEEE EMBS, 3*(1), 2675-2678. doi:10.1109/IEMBS.2003.1280467

Rong-Yi, Y., Zhong C. (2005). Blind source separation of multichannel electroencephalogram based wavelet transform and ICA. *Chinese Phys, 14*(11), 2176–2180. doi:10.1088/1009-1963/14/11/006

Roy, S., Kiral-Kornek, I. & Harrer, S. (2018) Deep learning enabled automatic abnormal EEG identification. *40th Annu.Int. Conf. IEEE Eng. Med. Biol. Soc. (EMBC),* 2756–2759. doi: 10.1109/EMBC.2018.8512756

Rugg, M.D. (2001). Event-related/Evoked Potentials. *International Encyclopedia of Social & Behavioral Sciences,* 4962-4966. doi:10.1016/B0-08-043076-7/03410-0

Rumelhart, D., Hinton, G., & Williams, R. (1986). Learning representations by back-propagating errors. *Nature, 323*(1), 533–536. doi:10.1038/323533a0

Safieddine, D., Kachenoura, A., Albera, L., Birot, G., Karfoul, A., Pasnicu, … Merlet, I. (2012). Removal of muscle artifact from EEG data: comparison between stochastic (ICA and CCA) and deterministic (EMD and wavelet-based) approaches. *EURASIP Journal on Advances in Signal Processing, 127*(1), 1-15. doi: 10.1186/1687-6180-2012-127

Sahu, M., Nagwani, N., & Verma, S. (2016). Applying auto regression techniques on amyotrophic lateral sclerosis patients EEG dataset with P300 speller. *Indian Journal of Science and Technology*, *9*(48), 1-8. doi:10.17485/ijst/2016/v9i48/109165

Sakhavi, S., Guan, C. & Yan, S. (2015). Parallel convolutional-linear neural network for motor imagery classification. *23rd European Signal Processing Conference (EUSIPCO)*, 2736-2740. doi:10.1109/EUSIPCO.2015.7362882

Salama, E.S. , El-Khoribi, R.A., Shoman, M.E. & Shalaby, M.A.W. (2018). EEG-based emotion recognition using 3D convolutional neural networks. *International Journal of Advanced Computer Science and Applications, 9*(8), 329–337. doi:10.14569/IJACSA.2018.090843

Satapathy, S.K, Dehuri, S. & Jagadev, A.K. (2016). ABC optimized RBF network for classification of EEG signal for epileptic seizure identification. *Egyptian Informatics Journal, 18*(1), 55–66. doi:10.1016/j.eij.2016.05.001

Scherg, M. & Berg, P. (1991). Use of prior knowledge in brain electromagnetic source analysis. *Brain Topography, 4*(2), 143-150. doi:10.1007/BF01132771

Schiff, S.J., Aldroubi, A., Unser, M. & Sato, S. (1994). Fast wavelet transformation of EEG. *Electroencephalography and Clinical Neurophysiology, 91*(6), 442–455. doi:10.1016/0013-4694(94)90165-1

Sharma, M., Pachori, R.B. & Acharya, U.R. (2017). A new approach to characterize epileptic seizures using analytic time-frequency flexible wavelet transform and fractal dimension. *Pattern Recognition Letters, 94*(1), 172-179. doi:10.1016/j.patrec.2017.03.023

Soleymani, M., Asghari-Esfeden, S., Pantic, M. & Fu, Y. (2014). Continuous emotion detection using EEG signals and facial expressions. *IEEE International Conference on Multimedia and Expo (ICME),* 1-6. doi:10.1109/ICME.2014.6890301

Somers, B. & Bertrand, A. (2016). Removal of eye blink artifacts in wireless EEG sensor networks using reduced-bandwidth canonical correlation analysis. *Journal of Neural Engineering, 13*(6); *066008*, 1-12. doi: 10.1088/1741-2560/13/6/066008

Subasi, A. & Gursoy, M.I. (2010). EEG signal classification using PCA, ICA, LDA and support vector machines. *Expert Systems with Applications, 37*(1), 8659-8666. doi:10.1016/j.eswa.2010.06.065

Supratak, A., Dong, H., Wu, C. & Guo, Y. (2017). DeepSleepNet: a model for automatic sleep stage scoring based on raw single-channel EEG. *IEEE Transactions on Neural Systems and Rehabilitation Engineering, 25*(11), 1998–2008. doi:10.1109/TNSRE.2017.2721116

Supratak, A., Li, L. & Guo, Y. (2014). Feature extraction with stacked autoencoders for epileptic seizure detection. *2014 36th Annual International Conference of the IEEE Engineering in Medicine and Biology Society,* 4184-4187. doi:10.1109/EMBC.2014.6944546

Tang, Z., Li, C. & Sun, S. (2017). Single-trial EEG classification of motor imagery using deep convolutional neural networks. *Optik-Int J Light Electron Opt*., *130*(1), 11-18. doi:10.1016/j.ijleo.2016.10.117

Thigpen, N., Kappenman, E., & Keil, A. (2017). Assessing the internal consistency of the event-related potential: An example analysis. *Psychophysiology, 54*(1), 123-138. doi:10.1111/psyp.12629

Thodoroff, P., Pineau, J. & Lim, A. (2016). Learning robust features using deep learning for automatic seizure detection. *Proceedings of the Machine Learning for Healthcare, 56*(1), 178-190. Retrieved from http://proceedings.mlr.press/v56/Thodoroff16.pdf

Tsinalis, O., Matthews, P.M. & Guo, Y. (2016). Automatic sleep stage scoring using time-frequency analysis and stacked sparse autoencoders. *Annals of Biomedical Engineering, 44*(5), 1587–1597. doi:10.1007/s10439-015-1444-y

Tsiouris, K.M., Pezoulas, V.C., Zervakis, M., Konitsiotis, S., Koutsouris, D.D. & Fotiadis, D.I. (2018). A long short-term memory deep learning network for the prediction of epileptic seizures using EEG signals. *Computers in Biology and Medicine, 99*(1), 24–37. doi: 10.1016/j.compbiomed.2018.05.019

Turnip, A. & Pardede, J. (2017). Artefacts removal of EEG signals with wavelet denoising. *MATEC Web of Conferences, 135*(6):*00058*, 1-10. doi: 10.1051/matecconf/201713500058

Ullah, I., Hussain, M., Qazi, E. & Aboalsamh, H. (2018). An automated system for epilepsy detection using EEG brain signals based on deep learning approach. *Expert Systems with Applications, 107*(1), 61–71. doi:10.1016/j.eswa.2018.04.021

Ungureanu, M., Bigan, C., Strungaru, R. & Lazarescu, V. (2004). Independent component analysis applied in biomedical signal processing. *Journal of the Institute of Measurement Science, 4*(2), Section 2, 1-8. Retrieved from http://www.measurement.sk/2004/S2/UNGUREANU.pdf

Vařeka, L. & Mautner, P. (2017). Stacked autoencoders for the P300 component detection. *Frontiers in Neuroscience, 11*(1); 302, 1-9. doi:10.3389/fnins.2017.00302

Vidyaratne, L., Glandon, A., Alam, M. & Iftekharuddin, K.M. (2016). Deep recurrent neural network for seizure detection. *2016 International Joint Conference on Neural Networks (IJCNN),* 1202–1207. doi:10.1109/IJCNN.2016.7727334

Vigário, R., Särelä, J., Jousmäki, V., Hämäläinen, M. & Oja, E. (2000). Independent component approach to the analysis of EEG and MEG recordings. *IEEE Transactions on Biomedical Engineering, 47*(5), 589-593. doi:10.1109/10.841330

Vincent, P., Larochelle, H., Bengio, Y. & Manzagol, P. (2008). Extracting and composing robust features with denoising autoencoders. In *Proceedings of the 25th International Conference on Machine Learning*, 1096–1103. doi:10.1145/1390156.1390294

Vorobyov, S. & Cichocki, A. (2002). Blind noise reduction for multisensory signals using ICA and subspace filtering, with application to EEG analysis. *Biol. Cybern. 86*(4), 293–303. doi: 10.1007/s00422-001-0298-6

Vrbancic, G. & Podgorelec, V. (2018). Automatic classification of motor impairment neural disorders from EEG signals using deep convolutional neural networks. *Elektronika Ir Elektrotechnika, 24*(4), 3-7. doi:10.5755/j01.eie.24.4.21469

Wang, M., Abdelfattah, S., Moustafa, N. & Hu, J. (2018). Deep gaussian mixture-hidden markov model for classification of EEG signals. *IEEE Transactions on Emerging Topics in Computational Intelligence*, *2*(4), 278-287. doi:10.1109/TETCI.2018.2829981

Wang, P., Jiang, A., Liu, X., Shang, J. & Zhang, L. (2018). LSTM-Based EEG classification in motor imagery task. *IEEE transactions on neural systems and rehabilitation engineering, 26*(11). 2086–95. doi:10.1109/TNSRE.2018.2876129

Wang, X., Gong, G., Li, N. & Qiu, S. (2019). Detection analysis of epileptic EEG using a novel random forest model combined with grid search optimization. *Frontiers in Human Neuroscience, 13*(52),1-13. doi:10.3389/fnhum.2019.00052

Wang, Z., Cao, L., Zhang, Z., Gong, X., Sun, Y. & Wang, H. (2017). Short time fourier transformation and deep neural networks for motor imagery brain computer interface recognition. *Concurrency Computat Pract Exper., 30*(1), 1-9. doi:10.1002/cpe.4413

Wei, X., Zhou, L., Chen, Z., Zhang, L. & Zhou, Y. (2018). Automatic seizure detection using three- dimensional CNN based on multi-channel EEG. *BMC Medical Informatics and Decision Making, 18*(111), 71-80. doi:10.1186/s12911-018-0693-8

Wen, T. & Zhang, Z. (2018). Deep convolution neural network and autoencoders-based unsupervised feature learning of EEG signals. *IEEE Access*, *6*(1), 25399-25410. doi:10.1109/ACCESS.2018.2833746

Xu, H. & Plataniotis, K.N. (2016). Affective states classification using EEG and semi-supervised deep learning approaches. *2016 IEEE 18th International Workshop on Multimedia Signal Processing (MMSP),* 1-6. doi:10.1109/MMSP.2016.7813351

Xun, G., Jia, X. & Zhang, A. (2016). Detecting epileptic seizures with electroencephalogram via a context-learning model. *BMC Medical Informatics and Decision Making, 16*(2), 97-109. doi:10.1186/s12911-016-0310-7

Xing, X., Li, Z., Xu, T., Shu, L., Hu, B. & Xu, X. (2019). SAE+LSTM: A new framework for emotion recognition from multi-channel EEG. *Frontiers in Neurorobotics*, *13*(37),1-14. doi:10.3389/fnbot.2019.00037

Yanagimoto, M. & Sugimoto, C. (2016). Recognition of persisting emotional valence from EEG using convolutional neural networks. *2016 IEEE 9th Int. Workshop Computational Intelligence Applications,* 27–32. doi:10.1109/IWCIA.2016.7805744

Yang, H., Han, J. & Min, K. (2019). A multi-column CNN model for emotion recognition from EEG signals. *Sensors, 19*(21); *4736*, 1-12. doi:10.3390/s19214736

Yang, B., Duan, K., Fan, C., Hu, C. & Wang, J. (2018). Automatic ocular artifacts removal in EEG using deep learning. *Biomedical Signal Processing and Control, 43*(1), 148-158. doi:10.1016/j.bspc.2018.02.021

Yang, B., Duan, K. & Zhang, T. (2016). Removal of EOG artifacts from EEG using a cascade of sparse autoencoder and recursive least squares adaptive filter. *Neurocomputing, 214*(1), 1053-1060. doi:10.1016/j.neucom.2016.06.067

Yang, Y., Wu, Q., Qiu, M., Wang, Y., & Chen, X. (2018). Emotion Recognition from Multi-Channel EEG through Parallel Convolutional Recurrent Neural Network. *2018 International Joint Conference on Neural Networks (IJCNN)*, 1-7. doi:10.1109/IJCNN.2018.8489331

Yao, Y., Plested, J. & Gedeon T. (2018). Deep feature learning and visualization for EEG recording using autoencoders. In Cheng L., Leung A. & Ozawa S. (eds), . Lecture Notes in Computer Science: Vol. 11307, *Neural Information Processing - ICONIP 2018* (pp. 554-566). Cham: Springer. doi:10.1007/978-3-030-04239-4_50

Yin, Z. & Zhang, J. (2017). Cross-session classification of mental workload levels using EEG and an adaptive deep learning model. *Biomedical Signal Processing and Control, 33*(1), 30–47. doi:10.1016/j.bspc.2016.11.013

Yu, Y., Si, X., Hu, C. & Zhang, J. (2019). A review of recurrent neural networks: LSTM cells and network architecture. *Neural Computation, 31*(7), 1235-1270. doi:10.1162/neco_a_01199

Yuan, Y., Xun, G., Jia, K. & Zhang, A. (2017). A multi-view deep learning method for epileptic seizure detection using short-time fourier transform. In *Proceedings of the 8th ACM International Conference on Bioinformatics, Computational Biology, and Health Informatics (ACM-BCB '17)*. Association for Computing Machinery, New York, NY, USA, 213–222. doi:10.1145/3107411.3107419

Zeng, H., Yang, C., Dai, G., Qin, F., Zhang, J. & Kong, W. (2018). EEG classification of driver mental states by deep learning. *Cognitive Neurodynamics, 12*(1), 597-606. doi:10.1007/s11571-018-9496-y

Zhou, W. & Gotman, J. (2008). Automatic removal of eye movement artifacts from the EEG using ICA and the dipole model. *Progress in Natural Science, 19*(1), 1165–1170. doi:10.1016/j.pnsc.2008.11.013

Zikov, T., Bibian, S., Dumont, G.A., Huzmezan, M. & Ries, C.R. (2002). A wavelet based de-noising technique for ocular artifact correction of the electroencephalogram. *Proceedings of the Second Joint EMBS/BMES Conference, 1*(1), 98-105. doi:10.1109/IEMBS.2002.1134407

Zou, Y., Nathan, V. & Jafari, R. (2016). Automatic identification of artifact-related independent components for artifact removal in EEG recordings. IEEE *Journal of Biomedical and Health Informatics, 20*(1), 73-81. doi:10.1109/JBHI.2014.2370646

APPENDIX A

Architecture 1

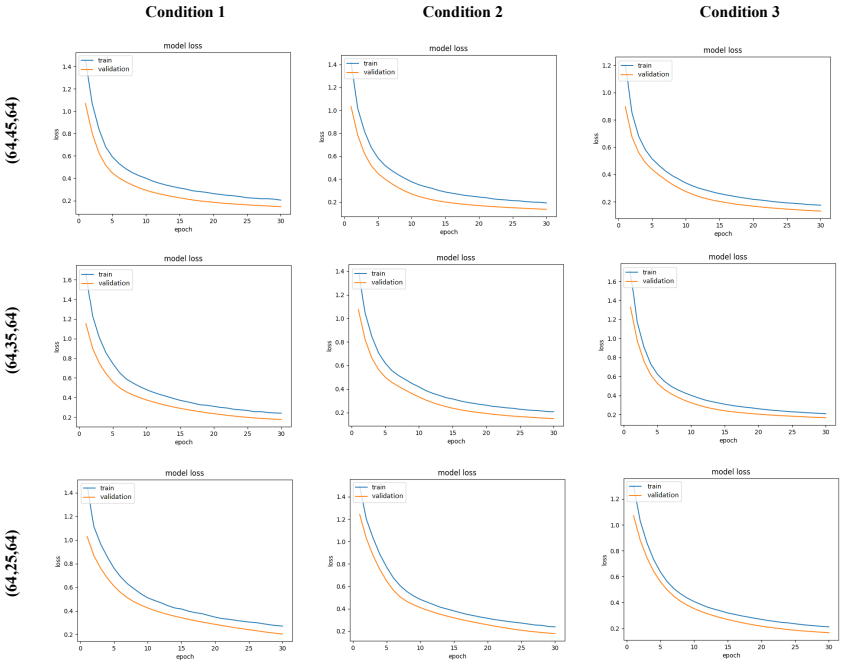

Training loss and validation loss changes during trainings for Architecture 1

Architecture 2

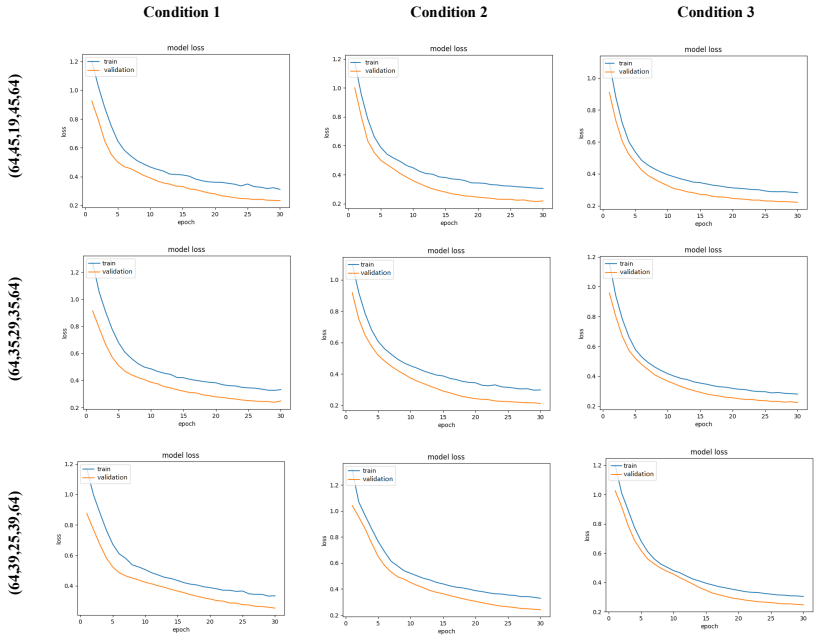

Training loss and validation loss changes during trainings for Architecture 2

Architecture 3

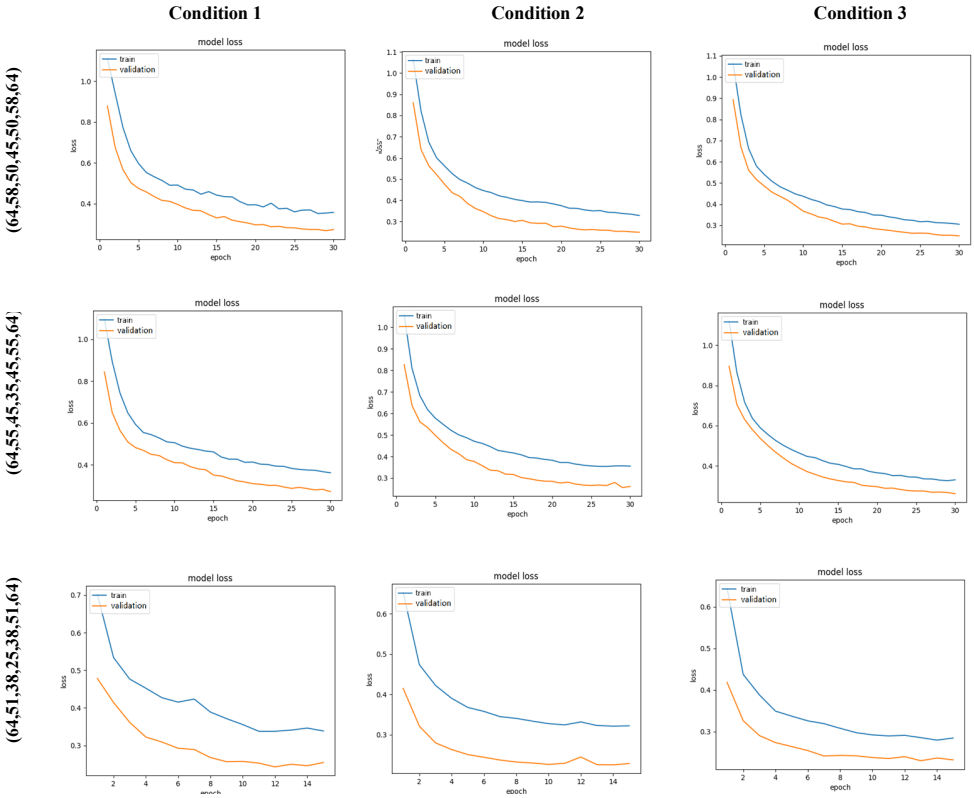

Training loss and validation loss changes during trainings for Architecture 3

APPENDIX B

Architecture 1 (64,35,64)

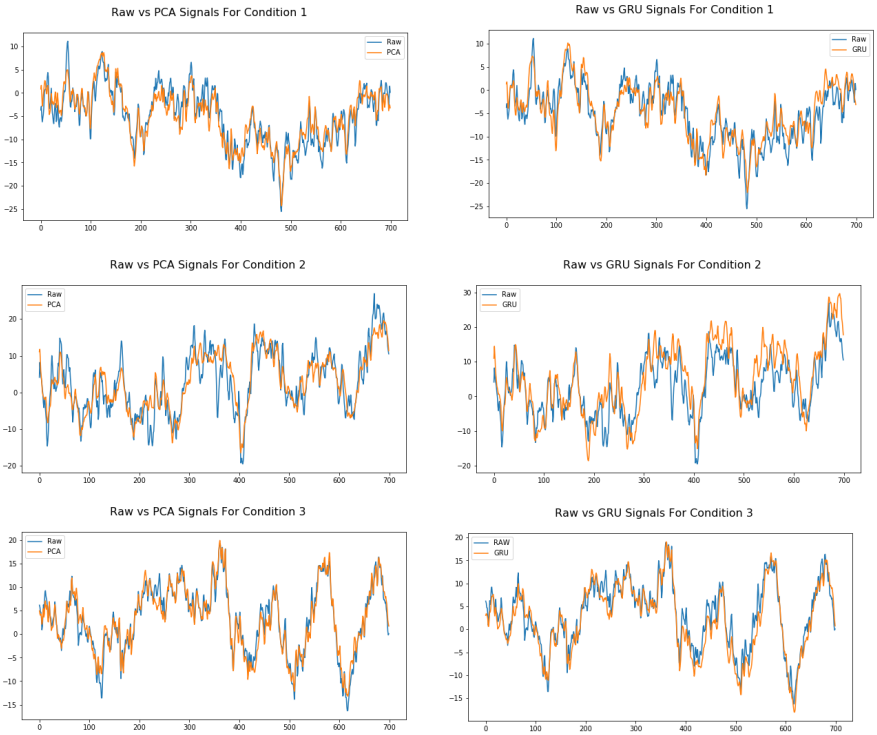

Raw signals vs PCA and GRU-AE reconstructed signals for each condition

Architecture 1 (64,25,64)

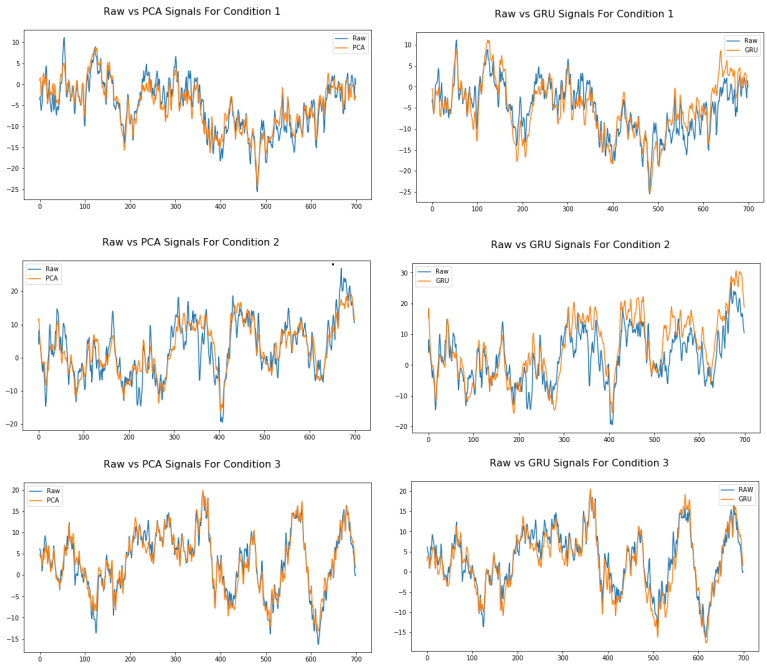

Raw signals vs PCA and GRU-AE reconstructed signals for each condition

APPENDIX C

Architecture 2(64,35,29,35,64)

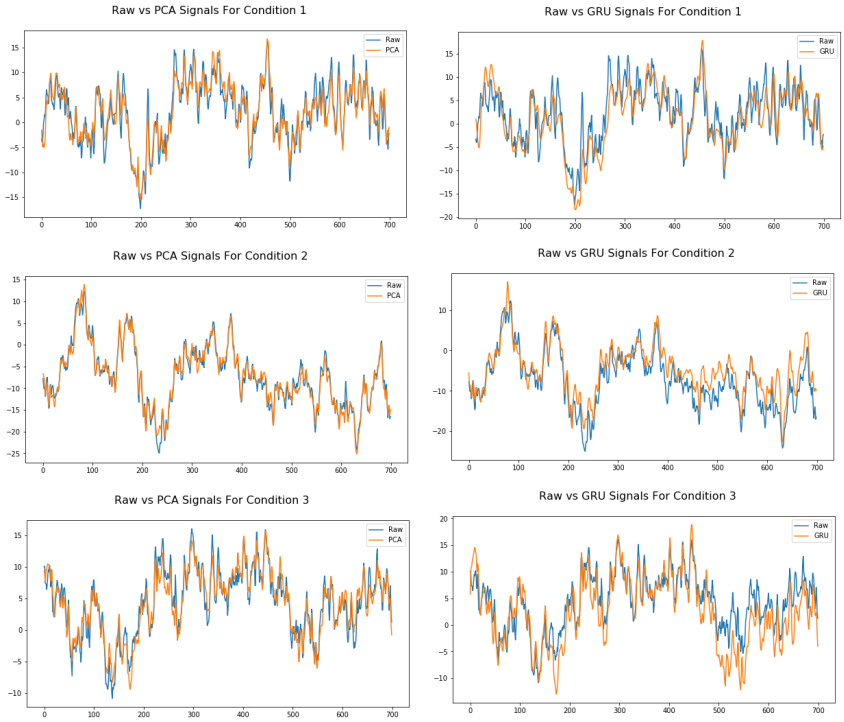

Raw signals vs PCA and GRU-AE reconstructed signals for each condition

Architecture 2(64,39,25,39,64)

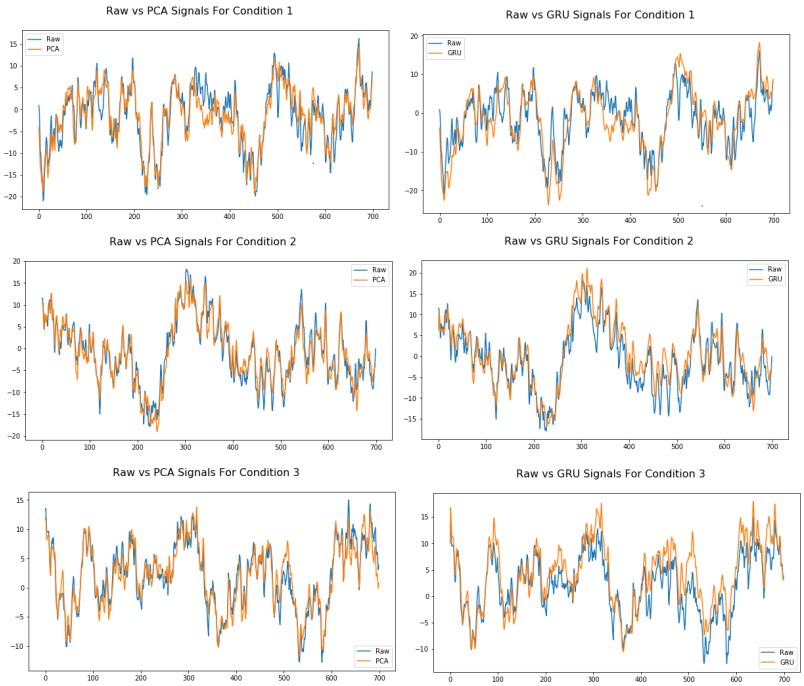

Raw signals vs PCA and GRU-AE reconstructed signals for each condition

APPENDIX D

Architecture 3 (64,55,45,35,45,55,64)

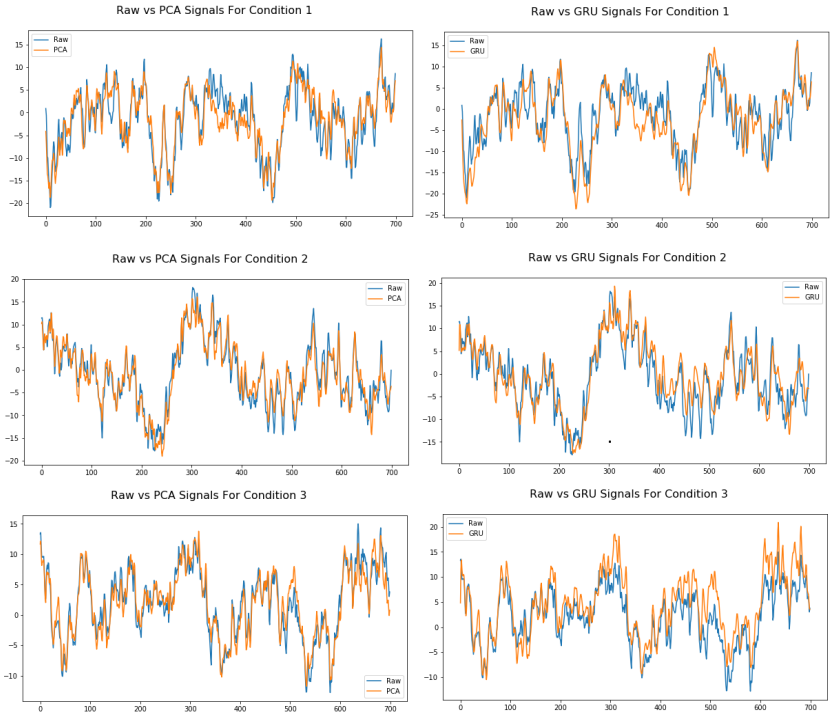

Raw signals vs PCA and GRU-AE reconstructed signals for each condition

Architecture 3 (64,51,38,25,38,51,64)

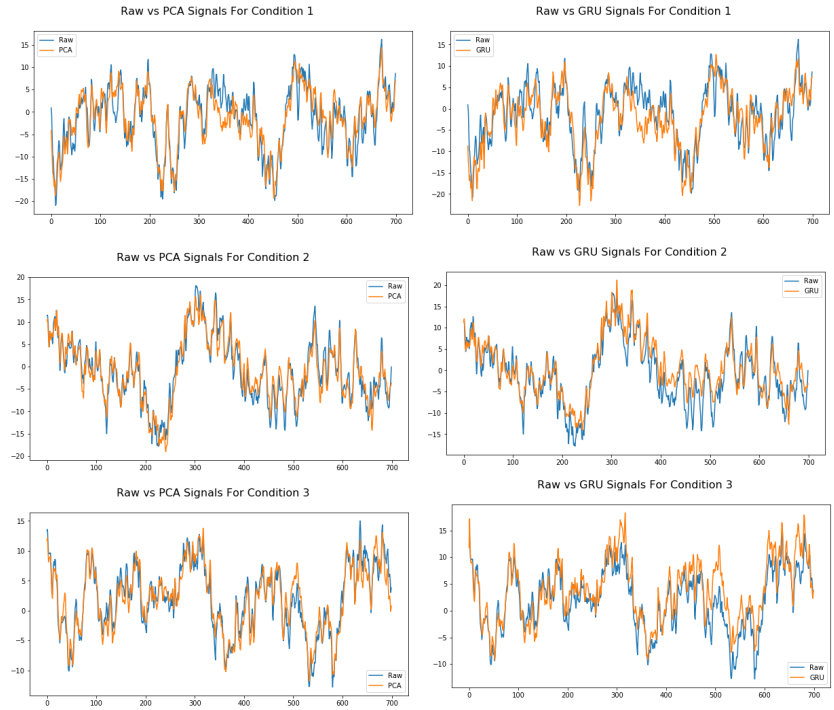

Raw signals vs PCA and GRU-AE reconstructed signals for each condition

APPENDIX E

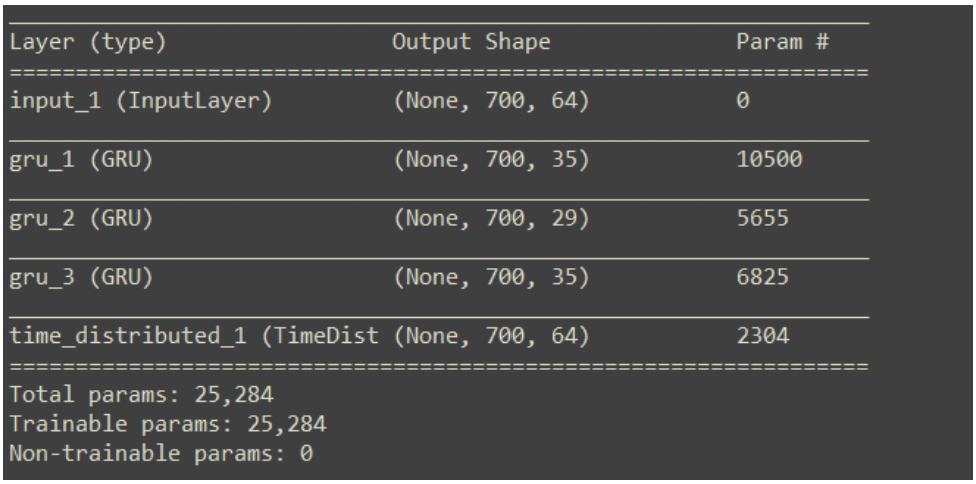

```
_________________________________________________________________
Layer (type)                 Output Shape              Param #
=================================================================
input_1 (InputLayer)         (None, 700, 64)           0
_________________________________________________________________
gru_1 (GRU)                  (None, 700, 35)           10500
_________________________________________________________________
gru_2 (GRU)                  (None, 700, 29)           5655
_________________________________________________________________
gru_3 (GRU)                  (None, 700, 35)           6825
_________________________________________________________________
time_distributed_1 (TimeDist (None, 700, 64)           2304
=================================================================
Total params: 25,284
Trainable params: 25,284
Non-trainable params: 0
```

Summary of the structure of the best model